Trends in Analytical Chemistry 191 (2025) 118346

Contents lists available at ScienceDirect

Trends in Analytical Chemistry

journal homepage: www.elsevier.com/locate/trac

Targeting hepatocellular carcinoma with aptamers: from biomarker detection to therapeutic applications

Magdolna Casian [a,b,c], Ioana Manea [a], Oana Hosu-Stancioiu [a], María Jesús Lobo Castañón [b,c], Noemí de-los-Santos-Álvarez [b,c,*], Cecilia Cristea [a,**]

[a] Department of Analytical Chemistry, Faculty of Pharmacy, Iuliu Haţieganu University of Medicine and Pharmacy, 4 Pasteur Street, 400349, Cluj-Napoca, Romania
[b] Departamento de Química Física y Analítica, Universidad de Oviedo, Av. Julián Clavería 8, 33006, Oviedo, Spain
[c] Instituto de Investigación Sanitaria del Principado de Asturias, Av. de Roma s/n, 33011, Oviedo, Spain

ARTICLE INFO

Keywords:
Aptamer
SELEX
Nanoparticles
Hepatocellular carcinoma biomarkers
Diagnostics
Drug delivery
Personalized medicine

ABSTRACT

Hepatocellular carcinoma (HCC) is one of the leading causes of cancer-related mortality worldwide, with a rising incidence, low-sensitivity screening methods, and resistance to conventional therapy. With the ongoing advancements in personalized medicine, aptamers have emerged as innovative biorecognition elements owing to high stability, versatile functionalization and cell internalization capability. This review provides a comprehensive overview of aptamers and their potential to address diagnostic and therapeutic gaps in HCC. Strategies for selecting aptamers targeting the most significant HCC biomarkers are discussed, along with their applications in HCC diagnosis and therapy. Examples include various innovative screening platforms and targeted delivery systems that incorporate the benefits of different nanomaterials. The advantages and limitations of aptamer-nanoconjugates are highlighted, along with the key requirements for translating these strategies into the clinical practice.

1. Introduction

Liver cancer is the sixth most frequently diagnosed cancer worldwide, with an age-standardized incidence rate of 8.6 per 100,000 people. It is also the third leading cause of cancer-related mortality globally (Fig. 1A and B). Moreover, the incidence of liver cancer is projected to rise by over 65 %, with global mortality expected to reach 1.26 million by 2045 [1]. Primary liver cancer originates within the liver and is classified based on cellular origin and pathological morphology. The two major types are hepatocellular carcinoma (HCC) and intrahepatic cholangiocarcinoma. In contrast, secondary liver cancer refers to malignancies that have metastasized to the liver from other organs, such as colorectal or pancreatic cancer [2]. HCC is the most prevalent type of liver cancer, accounting for approximately 90 % of all cases [3].

Chronic liver diseases, including hepatitis B and C infections, metabolic dysfunction-associated fatty liver disease, and cirrhosis are the primary drivers of HCC development [4,5]. Hepatitis B virus infection is the leading risk factor, responsible for approximately 50 % of all HCC cases [6], whereas the risk associated with hepatitis C virus infection has significantly declined due to effective antiviral treatments [7]. Furthermore, type 2 diabetes mellitus, obesity, and advanced age are well-established risk factors for the progression of fibrosis to cirrhosis [8]. Chronic liver inflammation, regardless of its cause, is a major predisposing factor for the development of primary liver cancer [2].

The increasing incidence and mortality of liver cancer cases pose a significant healthcare burden, necessitating innovative early-stage diagnostic and personalized treatment strategies [2]. The development of systematic evolution of ligands by exponential enrichment (SELEX) technology enabled the discovery of aptamers, high-affinity molecular binding agents selected from large nucleic acid libraries. This breakthrough expanded the functional potential of DNA and RNA oligonucleotides in cancer diagnosis and treatment. Aptamers provide several advantages, including ease of synthesis, reproducibility, simple chemical modification, high stability, and low immunogenicity [9]. Due to their small size and low molecular weight, aptamers can efficiently navigate and penetrate dense tumor matrices, which is essential for optimizing drug delivery dose and reducing adverse effects [10]. Despite their potential, aptamers face challenges such as nuclease degradation

* Corresponding author.
** Corresponding author.
E-mail addresses: santosnoemi@uniovi.es (N. de-los-Santos-Álvarez), ccristea@umfcluj.ro (C. Cristea).

https://doi.org/10.1016/j.trac.2025.118346
Received 11 May 2025; Received in revised form 17 June 2025; Accepted 18 June 2025
Available online 20 June 2025

and rapid renal clearance, which limit their *in vivo* stability and bioavailability. Overcoming these challenges is essential to unlock the clinical application [11,12]. According to Scopus, publications related to aptamers and HCC have shown growing interest from 1997 to 2024, with 11,258 publications recorded by November 2024 (Fig. 1C); these include studies focused on therapeutic and diagnostic applications.

This review provides a comprehensive overview of the potential application of aptamers in the early diagnosis and treatment of HCC. It highlights the benefits and challenges associated with using different SELEX strategies for the aptamer selection process and biomarker discovery, as well as the evolution of aptamer-nanoconjugates for diagnostic platforms and targeted therapy. Additionally, it presents aptamers that have progressed to clinical trials or reached the diagnostic market, emphasizing their translational potential.

2. HCC biomarkers: current insights in diagnosis and therapy

Despite advancements in imaging techniques and serum markers, early diagnosis of HCC remains challenging. Standard imaging methods, such as ultrasound, computed tomography (CT), and magnetic resonance imaging (MRI), often have limited sensitivity, particularly for small lesions or cirrhotic liver [13]. Consequently, molecular markers, including serum and tumor biomarkers, are highly valuable for improving the sensitivity and specificity of early HCC detection. Alpha-fetoprotein (AFP) is the most used biomarker for HCC surveillance and diagnosis, with serum levels typically ranging from 0 to 40 ng/mL in healthy adults but exceeding 400 ng/mL in HCC cases [2]. As the only phase V biomarker available for HCC screening, AFP is often combined with imaging techniques [14]. However, it is not ideal for early HCC detection because of its low specificity, as elevated levels can occur in liver cirrhosis as well as in gastric, pancreatic, and lung cancers. Additionally, its limited sensitivity poses a challenge, as some HCC patients do not secrete AFP [2]. To complement AFP, Des-γ-Carboxy Prothrombin (DCP) has been explored as an alternative marker, while its reliability is compromised in patients with vitamin K deficiency, malnutrition due to alcohol abuse, or those taking oral anticoagulants [15]. To address these limitations, a statistical model, the GALAD score, was developed by integrating sex, age, and blood levels of AFP, AFP-L3 (a fucosylated fraction of total AFP), and DCP to enhance HCC diagnosis and survival predictions [16].

Beyond AFP and DCP, other biomarkers show promise. Golgi protein-73 (GP-73), a transmembrane protein, offers superior sensitivity and specificity compared with AFP for early HCC detection. At a cut-off value of 35 ng/mL, GP-73 offered a sensitivity and specificity in detecting HCC as high as 74.6 % and 97.4 %, respectively [17]. Another promising marker, osteopontin (OPN), an integrin-binding phosphoprotein, has demonstrated better performance in differentiating early HCC from cirrhosis (75 % sensitivity and 62 % specificity) [18]. It also performs well in AFP-negative cases and combining OPN with AFP enhances the diagnostic accuracy [17].

Glypican-3 (GPC3) is a cell surface proteoglycan that is overexpressed in HCC but absent in normal or benign liver tissue, making it a valuable diagnostic biomarker. Immunohistochemical staining for GPC3 is increasingly used to differentiate HCC from other liver conditions [19]. At a diagnostic cut-off of 26.8 ng/mL, GPC3 has shown a sensitivity of 51.5 % and a specificity of 92.8 % [20]. However, clinical utility varies significantly depending on the detection method and the number of patients enrolled [21]. Another relevant biomarker, heat shock protein 70 (HSP70) is an oncogene that supports tumor survival and proliferation while inhibiting apoptosis [17]. These biomarkers, however,

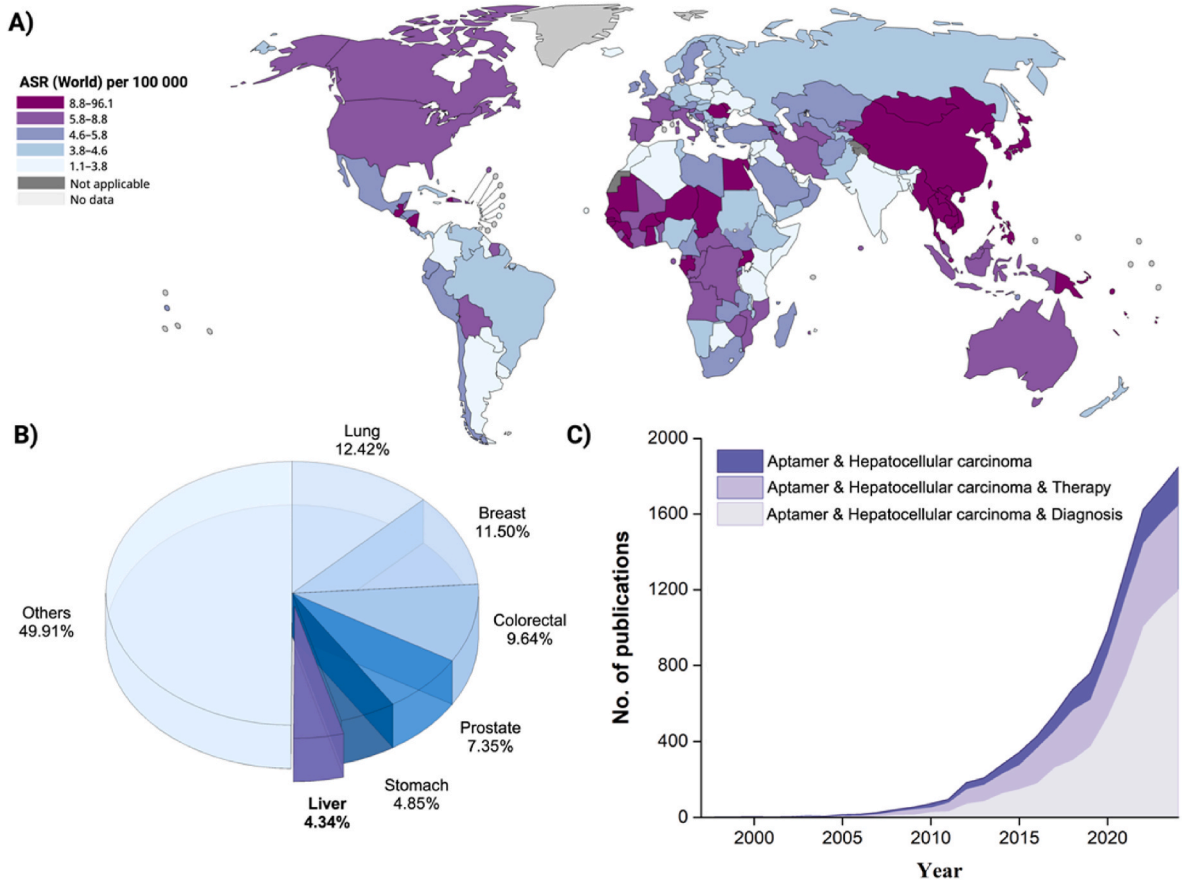

Fig. 1. Global liver cancer incidence: A) age-standardized incidence rate (ASR) per 100,000 population worldwide and **B)** percentages of the most prevalent cancer types, based on GLOBOCAN's 2022 report [1]. **C)** Publication trends in aptamer-based HCC research from 1997 to 2024, based on Scopus data.

are not universally expressed in all HCC cases. For instance, the European Association for the Study of the Liver recommends using GPC3, glutamine synthetase (GS), and HSP70 to identify dysplastic nodules and small HCCs (<2 cm) yet their combined sensitivity is only 25 %. Additionally, marker positivity varies by stage, with GPC3 being detected in 37.3 % of stage I, 71.9 % of stage II, and 92.9 % of stage III HCCs [2].

Dickkopf-1 (DKK-1), a secretory antagonist of the Wnt signaling pathway, has also been studied as a potential HCC biomarker, showing 50 % sensitivity and 80.8 % specificity when used alone. Other promising candidates include: endoglin (CD105), which is overexpressed in HCC microvessels and aids in quantifying tumor angiogenesis through microvascular density [22]; nucleolin, an oncogene involved in promoting cancer cell growth, proliferation, evasion of apoptosis and the immune system, metastasis, and angiogenesis [23]; lipocalin-2 (LCN2), which may aid in distinguishing HCC from liver cirrhosis [24], and galectin-1 (GAL-1), whose up-regulation is strongly associated with tumor adhesion, growth, migration, invasion, aggressiveness, metastasis, post-operative recurrence, and poor prognosis [25]. Table 1 provides a list of the most studied biomarkers for HCC diagnosis, including their sensitivity, specificity, and cut-off values. However, as previously mentioned, these parameters exhibit considerable variability due to methodological differences and patient heterogeneity.

Liquid biopsy is an appealing alternative to traditional tissue biopsy for cancer diagnosis and prognosis. This minimally invasive approach provides a more comprehensive view of tumor heterogeneity, is not operator-dependent, and allows for multiple sample collection to monitor tumor evolution in high-risk patients. Liquid biopsy targets include circulating tumor cells (CTCs), circulating tumor DNA (ctDNA), cell-free microRNA, and extracellular RNA [3,14]. Tumor-specific ctDNA methylation has demonstrated superior sensitivity and specificity compared to AFP, making it a valuable diagnostic and prognostic marker for HCC. However, using ctDNA for early surveillance requires highly sensitive sequencing technologies to identify low ctDNA levels in asymptomatic individuals, significantly increasing screening costs [14].

Despite significant progress in biomarker discovery for HCC, several limitations continue to hinder their routine clinical application. To date, only a few biomarkers have undergone rigorous prospective validation or received regulatory approval (AFP, AFP-L3 and DCP) thereby limiting the integration of other biomarkers into clinical guidelines [32]. The current lack of commercially available, fast and cost-effective tools for point-of-care biomarker analysis has significantly impeded the integration of personalized medicine into routine clinical practice [33]. To address the limitations of existing HCC biomarkers, recent technological advancements focus on the integration of multi-omics technologies for the identification of multi-dimensional biomarker panels (long non-coding RNA, microRNA, circulating RNAs, proteins, post translational modifications, metabolites), providing deeper insight into the molecular mechanism of HCC development and the integration of personalized medicine into routine clinical practice [34,35].

The effectiveness of HCC treatment is largely dependent on early diagnosis, as curative interventions such as surgical resection and ablation are most successful in patients with a low tumor burden and preserved liver function. However, recurrence rates remain high, necessitating additional treatment strategies. For intermediate-stage HCC, transarterial embolization and radiotherapy are common options, while systemic therapy is recommended for advanced-stage disease [3,14,36].

In advanced HCC, systemic therapies primarily include targeted treatments and immunotherapy [14]. Multikinase inhibitors such as sorafenib (SRF) and lenvatinib remain first-line therapies [3,14,37], while second-line options include regorafenib, cabozantinib, and the biomarker-guided therapy ramucirumab, which is approved for patients with AFP levels ≥400 ng/mL [3]. Immune checkpoint inhibitors (ICIs) like nivolumab and pembrolizumab offer new therapeutic avenues by reversing T-cell exhaustion [14], while combination regimens such as atezolizumab with bevacizumab have demonstrated superior overall survival compared to SRF [38,39]. Despite these advances, biomarker-driven treatment selection remains limited, and drug resistance challenges the long-term efficacy of these therapies [40,41].

Given the limitations of conventional treatments, aptamer-based therapies present a promising alternative. In the context of HCC, aptamers have been explored for targeting key oncogenic pathways, delivering cytotoxic agents, and improving the selectivity of imaging modalities. Their ability to bind to tumor-associated biomarkers such as GPC3 and AFP makes them valuable tools for both diagnosis and treatment.

Table 1
Key biomarkers for HCC diagnosis with sensitivity, specificity, and cut-off values.

Biomarker	Sensitivity (%)	Specificity (%)	Cut-off value	Ref.
AFP	61	81	20 ng/mL	[26]
DCP	74	86	40 mAU/mL	[27]
DKK-1	79.78	89.37	1.31 ng/mL	[28]
CD105	70	65	7.5 ng/mL	[29]
GP-73	74.6	97.4	35 ng/mL	[17]
GPC3	51.5	92.8	26.8 ng/mL	[20]
OPN	87.15	89.32	84.40 ng/mL	[30]
GS	73.6	98.2	599.3 ng/mL	[31]

3. SELEX innovations and HCC-biomarkers targeting

3.1. SELEX technology for in vivo applications

Traditional antibodies are widely regarded as the gold standard among biorecognition elements in both biosensing and therapeutic applications, owing to their natural ability to recognize and bind their targets with high selectivity [42]. However, they possess certain limitations such as susceptibility to degradation under high temperatures and pH variations, irreversible denaturation, very high molecular weight, and costly and time-consuming production via hybridoma technology which can generate batch-to-batch variability [43]. To address this challenges, alternative antibody-based biorecognition elements have been developed, such as antibody fragments and nanobodies. These engineered molecules offer advantages as reduced immunogenicity and improved access to certain hidden epitopes. However, these benefits often come at the cost of reduce binding affinity when compared to the full antibody [42,44].

The *in vitro* combinatorial synthesis by enrichment process, SELEX (Systematic Evolution of Ligands by EXponential enrichment), which was first introduced in 1990 by two independent groups [45,46], led to the discovery of aptamers. Aptamers exhibit antibody-like binding properties [47] and have emerged as powerful biorecognition elements in cancer research, offering innovative applications in both diagnostics and therapeutics.

Compared to antibodies, aptamers are smaller in size, can be stored in a wider range of solutions due to their chemical stability though they need nuclease-free conditions, easily synthesized *in vitro*, thus overcoming the ethical problems related to the use of animals for the *in vivo* production of antibodies. Moreover, they can be selected for a wide range of targets (including small molecules, ions, toxic compounds and non-immunogenic substances) and chemically functionalized with different functional groups or labels for various applications [43]. Their *in vitro* selection allows to tailor affinity and kinetic features without cell culture-associated artefacts. The 3D structure of aptamers, characterized by the formation of stems, inner rings, bulges, hairpins, pseudoknots, triplicates or G-quadruplex structures, enables highly specific interactions, with the formation of aptamer-target complex by complementary stacking, electrostatic forces, van der Waals interactions, and hydrogen bonding [48]. However, certain drawbacks of aptamers need to be addressed as well, such as reducing the selection time and cost of the SELEX technology, where the success or failure of aptamer discovery

can be assessed for individual aptamers only at the end of selection process, along with their susceptibility to nuclease-mediated degradation that can be alleviated by chemical modification in certain applications. The small size of aptamers can be sometimes disadvantageous, especially for *in vivo* imaging and targeted therapy, as it favors the rapid clearance from the bloodstream, in the same manner as for nanobodies [42,44].

The SELEX process consists of three primary steps: incubation, partitioning and amplification, as illustrated in Fig. 2A. Several key parameters influence selection process, including library design, selection stringency, generation of single-stranded nucleic acids, evolution of sequence enrichment, sequencing method and bioinformatics, and characterization method [49]. Through iterative rounds of selection, DNA/RNA sequences with binding affinities for the target of interest are isolated from a large library of oligonucleotides. Several challenges such as ineffective partition, PCR amplification bias, and even conformational changes (in either aptamer candidates or targets) can be encountered [50]. Incorporating counter-molecule competition using structural analogs enhances selection stringency, ideally enriching the candidates with the optimal binding affinities against the target molecule and enabling differentiation between structurally similar molecules, thus mitigating cross-reactivity events. For example, as the

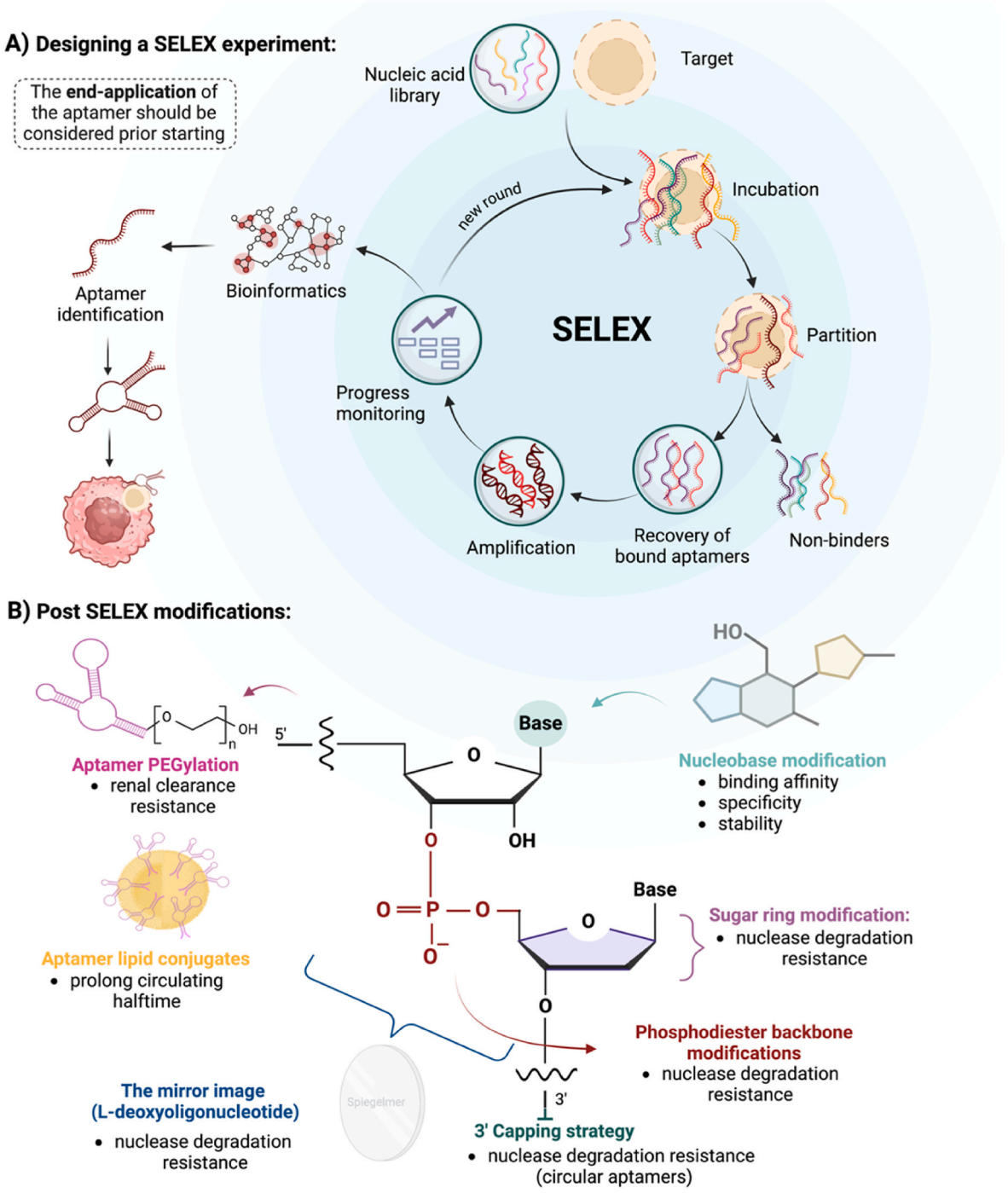

Fig. 2. A) The main steps of a typical SELEX experiment including incubation, partition, recovery, amplification, progress monitoring, bioinformatics, and aptamer identification, adapted from Ref. [49]. **B)** Common modification strategies of aptamers to increase the pharmacokinetic and pharmacodynamic properties, adapted from Ref. [56]. Created with Biorender.com.

initially selected cocaine-binding aptamer (with micromolar affinity) presented wide cross-reactivity with alkaloids and steroids, by implementing counter selection steps with testosterone, quinine and serotonin and truncation studies, new aptamers could be isolated specific to cocaine with a low nanomolar affinities, comparable with the best reported monoclonal antibody against cocaine [51]. Additionally, appropriate counter-selection steps or specific elution can direct the selection toward a target moiety. This feature of the SELEX makes aptamers an ideal receptor in the search for more specific biomarkers [52,53]. Reliable performance of aptamers relies on a thorough characterization of the binding affinity (K_D) and kinetics in a properly tailored environment that matches the intended application (e.g., artificial or real serum, whole blood, tumor environment etc.) [54]. Additionally, computational tools aid in secondary structure prediction, identifying critical structural motifs and regions capable of forming Watson–Crick base-pairing, further optimizing aptamer performance [55].

The SELEX strategies have evolved at the pace of technological advances. Improving the partitioning efficiency, from nitrocellulose filters [46] to magnetic beads (MBs) [57], capillary electrophoresis (CE) [58, 59], microfluidics [60] or particle display [61], has significantly reduced the production time from months to days, and the number of rounds to a single one on hydrogels [50]. Recent innovations like high-throughput instrumentation, high-efficient particle sorting and bioinformatics have achieved multiplex selection in a single SELEX without counter selection steps [62] or tuning the desire binding affinity [63]. Machine learning and computational tools are also guiding the aptamer discovery [64] and post-SELEX modification (truncation, multimerization) while deep learning approaches are able to predict the binding affinity [65].

Aptamers suffer from a short half-life *in vivo* and are prone to clearance from the body by kidney and nuclease digestion. Biochemical modifications at the sugar, base, or backbone levels, with molecules such as cholesterol, polyethylene glycol (PEG), 2′-amino pyrimidines, 2′-fluoro pyrimidines, etc. (Fig. 2B) can overcome these challenges to optimize their pharmacokinetics and biodistribution [66,67].

3.2. The selection of aptamers for HCC-related biomarkers

Starting from the extensively studied AFP biomarker, widely used in current clinical diagnostic protocols and for which four different aptamer selection studies have been reported [68–71], various additional HCC biomarkers have been investigated as potential targets in SELEX studies. To date, several aptamer sequences have been reported in the literature for biomarkers such as GP-73 [72], CD105 [73], GPC3 [74], DKK-1 [75], sialyl Lewis X (a carbohydrate aberrantly expressed in several types of circulating tumor cells) [76], LCN2 [77] and GAL-1 [78]. Furthermore, different HCC cell types have been explored as targets, including MEAR [79], metastatic HCCLM9 [80] and multidrug-resistant HCC cells [81], with one study advancing to the use of whole HCC serum [82] as a selection medium. The currently available SELEX studies presenting the selection of aptamers for HCC biomarkers and their affinities are summarized in Table 2 and Appendix A, respectively.

Following the traditional SELEX approach involving the immobilization of the target molecule on a carrier matrix [46], several strategies were applied, including solid phase-SELEX [72,73], MBs-SELEX [71, 75–78] or microfluidic MB-SELEX [69,70], where the target was bound to 96-well plates, sepharose beads or MBs, respectively. Some advantages of these strategies include the ease of separation, affordability and operational versatility [83]. Moreover, MBs are commercially available in a broad range of surface functionalizations and sizes, with some variants enabling oriented and specific target immobilization [84]. In the examples presented in Table 2, the amount of target used for MB functionalization was situated generally within the microgram range. However, the integration of microfluidic platforms with MB-based separation reduced the required target quantity to the nanogram scale. The limitations of target immobilization approaches include potential structural conformation changes of the target upon coupling, as well as the influence of the immobilization matrix, which may lead to nonspecific adsorption or steric hindrance affecting aptamer binding. These drawbacks can be partially mitigated by incorporating negative selection steps and using passivating agents in the selection buffer, such as Tween 20 or PEG [84,85].

An alternative SELEX approach commonly employed for large target molecules such as protein biomarkers is CE, which eliminates stationary support and linker biases by maintaining both the target and the oligonucleotide library free in solution. This technique enables direct separation based on differences in electrophoretic mobility upon complex formation, particularly useful when dealing with large, positively charged proteins [58]. CE-SELEX has been successfully applied to isolate aptamers against AFP [68] and GPC3 [74], requiring significantly fewer selection rounds compared to MB-SELEX (5 ± 1 vs. 11 ± 4 rounds). Additionally, CE-SELEX eliminates the need for extensive washing steps typical of traditional SELEX workflows, thus facilitating a more straightforward approach [58]. However, limitations of this method include the high cost of CE instrumentation, the need for specialized personnel and reduced library diversity due to the limited capillary load capacity [84].

With the ongoing advancements in personalized medicine and the expanding applications of aptamers in cancer diagnostics and targeted therapy, SELEX technology has evolved accordingly. Recognizing the complexity of cellular environment and the native conformation of biomarkers expressed on the cell surfaces, cell-SELEX was developed to enable the selection of aptamers using whole cells as targets. When opting for cell-SELEX, there is no need for prior protein purification, as well as no requirements for precise identification of the target on the cell surface, which can be explored for novel biomarker discovery [67,83]. This approach was effectively used to generate aptamers capable of specifically recognizing MEAR cell lines [79], as well as distinguishing between metastatic [80] and multidrug-resistant [81] HCC cell lines. To eliminate nonspecific interactions that could occur *in vivo*, all studies included counter selection steps using non-target cells. In contrast to the previously mentioned strategies, cell-SELEX technology generally required higher number of selection rounds (17 ± 7) and ongoing removal of dead cells to reduce nonspecific binding. These factors underscore several limitations of the method, including its time-consuming nature, high costs, and the need for advanced technical expertise for cell handling. A particularly innovative approach involved the use whole serum from HCC patients as the selection matrix, facilitating the clinical application of the resulting aptamers in HCC diagnosis [82]. This strategy could also aid in the discovery of new biomarkers that are not expressed on the cell surface but are instead present in the serum.

The composition of the selection buffer should be carefully tailored to its intended application, in order to promote the stability of aptamer secondary structures and enhance their binding properties. The most commonly used buffers for selecting HCC biomarker-specific aptamers include phosphate-buffered saline (PBS), tris(hydroxymethyl)aminomethane (TRIS) and 4-(2-hydroxyethyl)-1-piperazineethanesulfonic acid (HEPES). These buffers were enriched with various cations (Na^+, K^+, Ca^{2+}, Mg^{2+}) to facilitate proper folding and reduce electrostatic interactions and with molecules like bovine serum albumin and transfer RNA, imidazole or glucose to increase the selection stringency.

Recent advances in SELEX technologies have significantly improved the quality of the isolated aptamers, making them more suitable for detection, diagnostic imaging, and targeted drug delivery in cancer therapy [54]. However, despite their promising attributes, aptamers still face challenges in achieving target specificity in complex biological environments, limiting their clinical applications. To facilitate their translation into human clinical trials, improvements in biocompatibility, stability and bioavailability are essential. Aptamers can serve as efficient targeting agents in drug delivery vehicles, capable of transporting proteins, drugs or nucleic acids to specific cells through conjugation with

Table 2
Aptamer screening strategies targeting HCC biomarkers reported in the literature.

Target	Name	Aptamer type	Type of SELEX	Enrichment monitoring	Binding buffer	Number of rounds		Selectivity		Effect (*in vitro/in vivo*)	Ref.
						Total	Max. enrichment	Target (+) cells	Target (−) cells		
Alpha fetoprotein	AP273	DNA	CE-SELEX	CE based laser induced fluorescence detection system	30 mM NaH_2PO_4 pH 7.5	4	4	HepG2	SMMC7721, A549	Inhibition of HCC cell migration and invasion (*in vivo*)	[68]
	AFP-Apt1	DNA	Microfluidic MB-SELEX	SDS-PAGE	PBS pH 7.4 + 1 % BSA	6	6	–	–	–	[69]
	AFP-Apt 2	DNA	Microfluidic MB-SELEX	SDS-PAGE	PBS pH 7.4 + 1 % BSA	5	5	–	–	–	[70]
	Group I_17	RNA	MB-SELEX	Semi-quantitative real-time PCR	30 mM Tris–HCl, pH 7.5 + 150 mM NaCl + 1.5 mM $MgCl_2$ + 2 mM dithiothreitol +1 % BSA	16	16	HepG2, Hep3B, SK-Hep1, Huh7	HT29, NIH-3T3, AGS, HL-60, MCF7	Inhibition of AFP-induced oncogene mRNA overexpression and prevention of HCC proliferation (*in vitro*)	[71]
Golgi Protein 73	A10-2	DNA	Solid-phase SELEX	Enzyme-linked aptamer sorbent assay	20 mM HEPES + 120 mM NaCl + 5 mM KCl + 1 mM $CaCl_2$ + 1 mM $MgCl_2$ pH 7.3	10	10	HepG2, MCF7, MDA-MB-231, MDA-MB-435, A549	Normal liver tissue	–	[72]
Endoglin (CD105)	Apt1	DNA	Solid-phase SELEX	NA	NA	8	8	HUVECs SMMC7721	MCF7, NCTC 1469	–	[73]
Glypican 3	AP613-1	DNA	CE-SELEX	NA	30 mM NaH_2PO_4 pH 7.5	6	6	Huh7	A549	–	[74]
Dickkopf-1	34 del	DNA	MB-SELEX	Ni-NTA-MBs binding assay	PBS + 5 mM $MgCl_2$ + 5 mM imidazole + 1 % BSA + 1 μg/mL t-RNA + 0.02 %(v/v) Tween-20 pH 7.4	5	5	–	–	–	[75]
Sialyl Lewis X	sLeX-AP	DNA	MB-SELEX	NA	0.2 M Tris-HCl pH 7.4 + 1.37 M NaCl + 25 mM $MgCl_2$ + 100 mM dithiothreitol	12	12	HepG2	–	–	[76]
Lipocalin-2	LCN2_apta2 LCN2_apta4	DNA	MB-SELEX	UV-VIS spectroscopy Real-time PCR	500 mM NaCl + 20 mM Tris-HCl + 5 mM imidazole pH 7.9	10	8	–	BSA, GST, HSA, AFP	–	[77]
Galectin-1	Ap-74 M-545	DNA	MB-SELEX	NA	PBS + 2.95 mM KCl + 1 mM $MgCl_2$ + 2.4 mM $CaCl_2$ + 0.1 % Tween 20 + 10 mM imidazole pH 7.0	10	10	Jurkat T	–	Tumor growth suppression	[78]
MEAR cell	TLS11a TLS9a	DNA	Cell-SELEX	Flow cytometry	DPBS + 4.5 g/L glucose + 5 mM $MgCl_2$ + 0.1 mg/mL t-RNA +1 mg/mL BSA	16	16	MEAR	H23, Huh7, K562, Jurkat, Ramos, CCRF-CEM	–	[79]
Metastatic HCCLM9 cell	LY-1	DNA	Cell-SELEX	Flow cytometry Immunofluorescence imaging	PBS + 1 M $MgCl_2$ + 0.1 mg/mL t-RNA +1 mg/mL BSA + 1 mg/mL Salmon sperm DNA	11	9	HCCLM9	MHCC97L, HepG2, Huh7	Inhibition of cell migration (*in vitro*) In-vivo tumor growth suppression	[80]
Multidrug-resistant HCC cell	PS-ZL-7c	DNA	Cell-SELEX	Flow cytometry	DPBS + 4.5 mg/mL glucose + 5 mM $MgCl_2$ + 1 mg/mL BSA + 1 mg/mL t-RNA	25	25	HepG2/MDR	L02, HepG2	–	[81]
HCC serum	Ap–HCS–9-89 Ap–HCS–9-90	DNA	Whole serum-SELEX	PAGE	20 mM HEPES-Na^+ + 120 mM NaCl + 5 mM KCl + 1 mM $CaCl_2$ + 1 mM $MgCl_2$ pH 7.35	9	9	–	Normal serum	–	[82]

A549 - Human lung cancer line (glypican3 negative); AFP - Alpha fetoprotein; AGS - Non-hepatocellular carcinoma cell line; Apt – Aptamer; BNL CL.2 - Normal mouse liver cell line; BSA - Bovine serum albumine; CCRF-CEM - Human leukemia cell line; CE - Capillary electrophoresis; CTC - Circulating tumor cell; DPBS - Dulbecco's phosphate-buffered saline; GPC3 - Glypican 3; GST - Glutathione S-transferase; H23 - Human lung cancer cell line; HCC - Hepatocellular carcinoma; HCCLM9 - Hepatocellular carcinoma cell line with high metastatic potential; Hep3B - Hepatocellular carcinoma cell line; HEPES - 4-(2-hydroxyethyl)-1-piperazineethanesulfonic acid; HepG2 - Human hepatocellular carcinoma cell line; HL-60 - Non-hepatocellular carcinoma cell line; HSA - Human serum albumin; HT29 - Non-hepatocellular carcinoma cell line; Huh7 - Human liver cancer cell line (glypican3 positive); HUVECs - Endoglin expressed cell line; Jurkat - Human leukemia cell line; K562 - human leukemia cell line; Kato III - Human gastric carcinoma cell line; L02 - Human normal hepatocyte cells; MB - Magnetic beads; MCF7 - Golgi protein 73 expressed cell lines; MDA-MB-231 - Golgi Protein 73 expressed tumor cell line; MDA-MB-435 - Golgi protein 73 expressed tumor cell line; MEAR cells - MHCC97 - Hepatocellular carcinoma cell line with low metastatic potential; mRNA - Messenger RNA; NCTC 1469 - Murine normal liver cell line; NIH-3T3 - Non-hepatocellular carcinoma cell line; PAGE – Polyacrylamide gel electrophoresis; PBS - Phosphate-buffered saline; PCR - Polymerase chain reaction; Ramos - Human lymphoma cell line; RNA - Ribonucleic acid; SDS-PAGE - Sodium dodecyl sulfate polyacrylamide gel electrophoresis; SK-Hep1 - Hepatocellular carcinoma cell line; SMMC7721 - Human hepatoma cell line; Tris - Tris(hydroxymethyl)aminomethane; t-RNA - Transfer ribonucleic acid; UV-VIS - Ultraviolet–visible.

nanoparticles and/or drug molecules or small interfering RNAs (siRNAs), potentially improving patient compliance with treatment [66]. The conjugation of aptamers with other biomolecules, including other aptamers, siRNAs, proteins, enzymes, imaging agents, and therapeutic drugs, has led to the development of chimeric aptamers. These multifunctional aptamers hold the potential to revolutionize both cancer diagnostic and treatment strategies [86].

4. Nanoparticles and aptamer conjugation

The complexity of the tumor microenvironment, combined with individual variations, poses significant challenges in developing effective treatments for cancers, including HCC [87]. This has driven the need for innovative drug delivery strategies. Nano-sized particles or materials, composed of biocompatible and biodegradable substances, can efficiently deliver proteins, peptides, or nucleic acids to specific cells [66].

Smart nanoparticles (NPs) represent a major advancement in cancer therapy due to their stimulus-responsive and targeted drug delivery

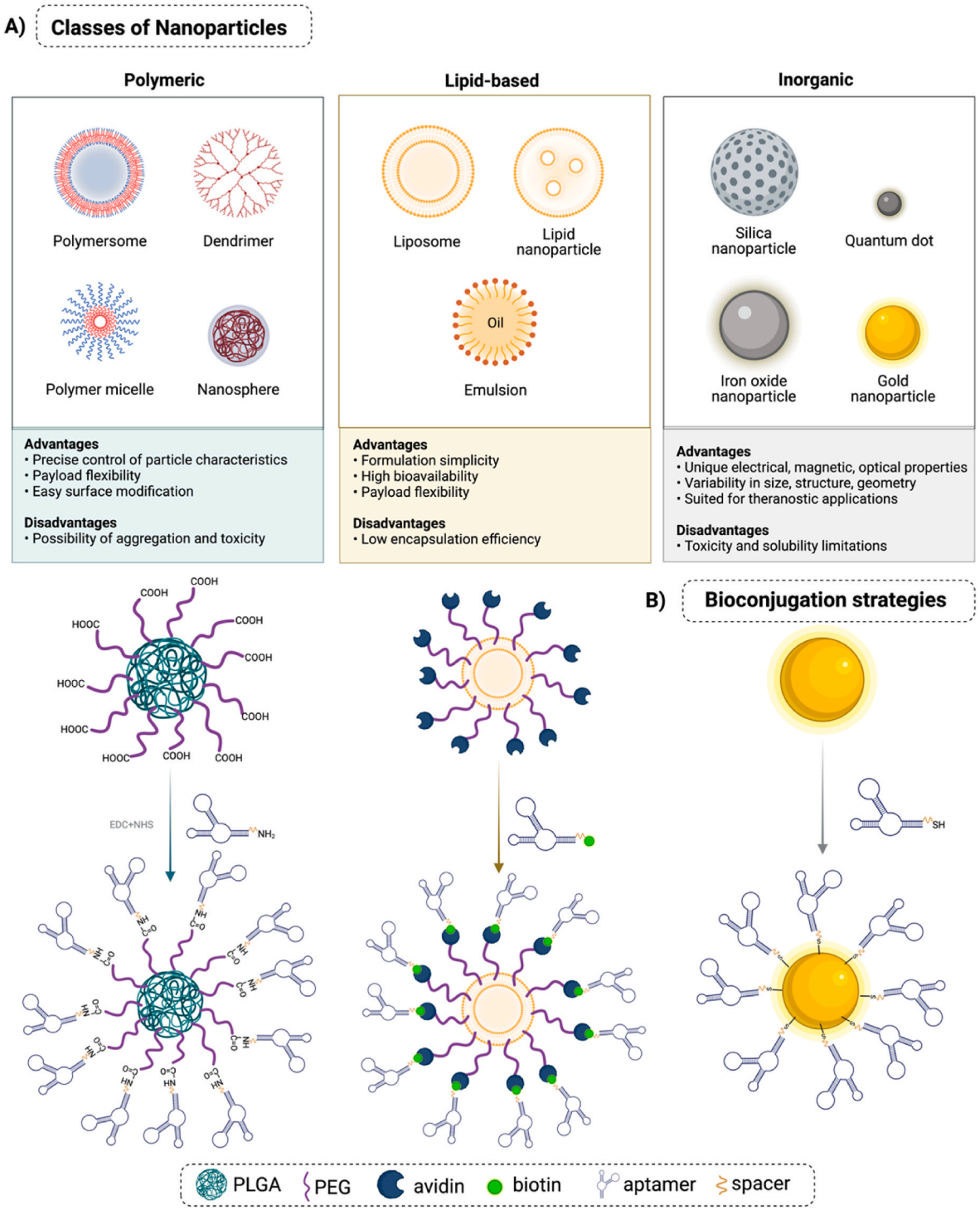

Fig. 3. A) Nanoparticle classes used for diagnostics and targeted therapy applications, along with their main advantages and limitations, adapted from Ref. [89]. **B)** Nanoparticle type-based aptamer bioconjugation strategies, adapted from Ref. [106]. Created with Biorender.com.

capabilities. These nanocarriers can adjust their size, shape, surface properties, and composition in response to endogenous or exogenous stimuli, such as enzymes, pH, temperature, light, and magnetism. Additionally, their ability to co-deliver therapeutics and diagnostic agents has significantly enhanced cancer theranostics [88,89].

An ideal smart NP should meet key characteristics, including stimulus-responsive properties, stable nanometer-scale size, adjustable surface charge, high encapsulation efficiency, biocompatibility, degradability, and low toxicity [89]. Nanocarriers can be grouped into three categories: (i) polymer-based, including polymeric NPs, dendrimers, and micelles; (ii) biomimetic-based, comprising liposomes, protein NPs, and cell membrane-coated NPs; and (iii) inorganic-based, which includes mesoporous silica NPs (MSiNPs), gold NPs (AuNPs), iron oxide (Fe_3O_4) NPs, quantum dots (QDs), carbon nanotubes, as well as advanced smart nanocarriers like black phosphorus quantum dots (BPQDs) and metal-organic frameworks [89]. Each type of nanocarrier has distinct properties (as shown in Fig. 3A), allowing for selection based on the drug type and treatment needs. For instance, micelles are well-suited for delivering water-insoluble or amphiphilic drugs, while liposomes enhance cellular uptake [90,91]. Functionalization, such as PEGylation, improves stability and prolongs circulation by evading the reticuloendothelial system [89,92].

Inorganic nanocarriers generally consist of a core (gold, QDs, silica, or Fe_3O_4) and a shell (organic polymers, metals or semiconductors), which facilitates biomolecule conjugation and shields the core from unwanted biological interactions or improves optical features. Their magnetic, optical and plasmonic properties make them valuable as contrast agents in MRI, CT, or positron emission tomography (PET) imaging [93,94]. Among them, zero-dimensional (0-D) fluorescent nanoparticles, like QDs, are promising for targeted drug delivery, real-time monitoring, and *in vivo* molecular imaging due to their unique properties, such as small size, large surface area, biocompatibility, tunable photoluminescence, and resistance to photobleaching [95]. However, their hydrophobic nature, tendency to aggregate, and non-specific adsorption are challenges that must be faced [96]. To improve water solubility and bioactivity, QDs are coated with polar species or ligand shells, enabling to encapsulate hydrophobic drugs while immobilizing hydrophilic agents and targeting molecules for multifunctional applications [95]. Two-dimensional (2-D) layered double hydroxides (LDHs), also known as hydrotalcite-like compounds, have gained interest as drug delivery carriers due to their adjustable drug release rates by modifying interlayer anions. LDHs consist of positively charged layers of divalent (e.g., Mg^{2+}, Ca^{2+}, Ni^{2+}) and trivalent (e.g., Al^{3+}, Cr^{3+}, Fe^{3+}) metal ions, balanced by interlayer anions like Cl^-, NO_3^-, or CO_3^{2-} [97]. Anionic drugs and biomolecules (e.g., genetic materials, peptides, proteins) can be intercalated into these layers, providing protection from enzymatic degradation in biological fluids [95]. AuNPs, with their large surface area and versatile binding capacity, are widely used in sensing, imaging, and therapy [89]. Despite their advantages, the therapeutic success of inorganic nanoparticles is often limited by low drug-loading capacity and significant toxicity [98]. The NPs toxicity is strongly linked to their physicochemical characteristics, particularly their size, shape, coating, solubility and surface charge, which significantly influence their biological interaction, tissue distribution, uptake by lymphatic or blood components, and their clearance efficiency. Smaller NPs (<10 nm) are typically excreted rapidly via the renal pathway, thereby reducing their circulation time in the bloodstream. In contrast, larger NPs (>200 nm) tend to accumulate more readily in highly vascularized organs, such as liver and spleen [99,100]. For *in vivo* applications, the optimal size of magnetic NPs should be situated within 15–100 nm diameter range [101]. Surface characteristics also influence nonspecific interactions, as positively charged NPs can adsorb to the negatively charged cell membrane promoting endocytosis and subsequent accumulation in cells [102].

Long-term exposure to inorganic NPs has been typically linked with inflammation, fibrosis and impaired clearance, although some nanomaterials have some more specific toxicological mechanisms. For example, exposure to Fe_3O_4 NPs triggers the induction of oxidative stress which can affect endothelial barrier permeability [103], while SiO_2 NPs are associated with metabolic disturbances due to aberrant protein expression [99]. AuNPs can selectively accumulate at vascular inflammation regions and potentially increase the risk of vascular disease and atherosclerosis events. Moreover, they have prolonged retention time in the body, being detected in blood and urine up to three months after exposure [104].

The most frequently employed strategies envisioned to reduce the potential cytotoxicity of inorganic NPs consist of coating their surface with biopolymers such as PEG and chitosan, thus enhancing biocompatibility and renal excretion [105]. Given the broadness of this field, more details can be found in the following review articles [89,95,98].

Combining aptamers, which specifically recognize tumor antigens or biomarkers, with nanoparticles enables active tumor targeting of anticancer drugs while minimizing the toxicity to normal tissues. Modifying HCC-specific aptamers onto nanomaterials enhances their clinical potential by increasing *in vivo* stability, protecting them from enzymatic degradation and rapid renal clearance, and improving target specificity [11,66]. This dual action enhances drug penetration, reduces off-target interactions, and boosts treatment efficacy, creating new opportunities for personalized cancer medicine [11]. Bioconjugation strategies widely applied for aptamer grafting onto NPs primarily rely on amide or Au-thiol covalent bonds and the specific avidin-biotin interaction, as shown in Fig. 3B.

5. Application of aptamers in cancer diagnosis

High-affinity aptamers, with low K_D (where the association rate exceeds the dissociation rate), enable rapid target binding and low detection limits, making them ideal for point-of-care diagnostic applications. Conversely, low affinity oligonucleotides with high K_D (where the dissociation rate dominates) exhibit fast binding kinetics, allowing for real-time monitoring of dynamic analyte changes [54,63]. Moreover, for biosensing applications, it is crucial that the linear detection range aligns with the relevant sensing window to ensure accurate and reliable diagnostics [54]. This section will discuss various biosensors integrating aptamers specific to HCC biomarkers and NPs to enhance detection sensitivity. Table 3 summarizes key aspects of these biosensors, including sensing platform configurations, detection methods, limits of detection (LOD), linear ranges, and interference studies, while Appendix B provides the primary structures of the aptamers used in these studies.

5.1. Sensing platforms for detecting AFP

AFP is the primary biomarker for HCC surveillance and diagnosis, driving the development of numerous sensing platforms for its quantification [107–121]. Among the various nanomaterials utilized in these designs, AuNPs are the most extensively employed, enabling highly sensitive detection across multiple transduction modalities. Electrochemical aptasensors have been particularly well studied for AFP detection. One of the first electrochemical aptasensor featured an AFP aptamer immobilized on a gold electrode (AuE) functionalized with spindle-shaped gold nanostructures, achieving detection in the nM range via differential pulse voltammetry (DPV) [107]. Li *et al.* reported another label-free electrochemical aptasensor using a screen-printed carbon electrode (SPCE) that incorporated thionin (TH), reduced graphene oxide (RGO), and AuNPs. All these materials were assembled by electrostatic interactions. The recognition of the AFP increases the TH redox current measured by DPV, but the detection range is not enough to detect AFP in serum from healthy people [108]. The same group proposed a light-addressable potentiometric sensor (LAPS) method with marginally improved performance. [109]. Zhao *et al.* proposed a chiroplasmonic assay, in which an AFP aptamer hybridized with its complementary sequence immobilized on different AuNPs, leading to the

Table 3
Sensing platform configurations for HCC biomarker quantification reported in the literature.

Target biomarker	Metalic nanoparticle	Platform	Detection method	LOD	Linear range	Selectivity studies	Real sample analysis	Incubation time (min)	Ref.
AFP	Au	AuE/sAuNPs/Apt_{AFP}/MCH	DPV	0.23 pg/mL	0.005–10 ng/mL	IgG, CEA, BSA, HSA	Human serum	42	[107]
		SPCE/AuNPs/RGO/TH/Apt_{AFP}	DPV	0.050 μg/mL	0.1–100 μg/mL	IgG, IgE, BSA, HSA	Human serum	60	[108]
		$LAPS_{chip}$/MPTES/AuNPs/Apt_{AFP}/BSA	LAPS	92.0 ng/mL	0.1–100.0 μg/mL	IgG, IgE, BSA, HSA	Human serum	60	[109]
		AuNP/cDNA-1@Apt_{AFP}@cDNA-2/AuNP	CD	11 pg/mL	0.02–5 ng/mL	PSA, HSA, THR, Tel, MTase, IgA	Human serum	60	[110]
		QDs-AuNPs/Apt_{AFP}	FRET	400 pg/mL	0.5–45 ng/mL	BSA, HSA, IgG, CEA	Spiked human serum	80	[111]
		LFD: CoP: AuNP/Det-Apt TP: Strep-Biot/Cap-Apt CL: Strep-Biot/Con-Sequence	Colorimetric	10 ng/mL	10–100 ng/mL	–	Human serum	10	[112]
	Au, Pt	SPCE/Au-PtNPs/RGO–CS–Fc/Apt_{AFP}/BSA	DPV	0.3013 ng/mL	0.001–10.0 μg/mL	HSA, IgG, IgE	Human serum	60	[113]
	Pt	SPCE/GO-COOH/PtNPs/Apt_{AFP}/BSA	SWV	1.22 ng/mL	3.0–30 ng/mL	PSA, BSA, IgG, HBsAg	Human serum	45	[114]
	Pd	PdNPs/Apt_{AFP}	FRET	1.4 ng/mL	5.0–150 ng/mL	BSA, HSA, IgG, IgE	Spiked diluted human serum	70	[115]
	Ni	SPCE/N-Cn-box@$Ni(OH)_2$/Apt_{AFP}/BSA	EIS	0.3 fg/mL	1 fg/mL – 100 ng/mL	CEA, HCG, PSA, IgG, IgE, MUC1, HER2, PTK7	Human serum	60	[116]
	–	RCDs/Apt	Fluorescence	3.5 pg/mL	0.01 ng/mL - 105 ng/mL	CEA, CA15-3, CA125, BSA, TT, TYR, DA, NE, ATP, FA, CLU, Vit B1, Vit B2, Vc, Fe^{3+}, Ca^{2+}, Na^{+}, K^{+}	Human serum	10	[117]
	–	FTOG/TiO_2/In_2S_3/CDs/Apt/BSA	PEC	5.1 pg/mL	0.002–100 ng/mL	CEA, PSA, IgG, AA	Human serum	NA	[118]
	Ag	AgNPs/Apt_{AFP} AgNPs/cDNA–1 AgNPs/cDNA–2	SERS	0.097 aM	0.2–20 aM	PSA, HSA, IgG, THR, MUC-1, VEGF	Human serum	30	[119]
	Au, Ag	AuNPs@MBIA@AgNPs@Apt&cDNA-Cy3	SERS	3.8 pg/mL	0.0038–100 ng/mL	HSA, BSA, THR, IgG	Human serum	90	[120]
	Au	Au–Au–UCNP/Apt_{AFP}&Apt_{MUC1}	SERS	0.059 aM	1–100 aM	PSA, HSA, BSA, IgG, THR	Human serum	600	[121]
GP73	–	MoS_2@N–GQDs/Apt_{GP73}	FRET	1.29 ng/mL	2.5–100 ng/mL	AFP, HSA, IgG, IgE	Human serum	80	[122]
	–	MoS_2@RGO/N–GQDs/Apt_{GP73}	FRET	4.59 ng/mL	5–100 ng/mL	BSA, HSA, IgG, IgE	Human serum	60	[123]
	–	SPCE/AuNPs/Apt_{A10-2}/BSA MoS_2-PANI@Fc/Apt_{GP73-1}	DPV	0.001 ng/mL	0.001–100 ng/mL	AFP, BSA, HSA, IgG, LDL	Human serum	40	[124]
	Pd	N-GQDs/Apt_{GP73}/MoS_2-Fc-PdNPs	FRET DPV	0.812 ng/mL 0.0425 ng/mL	1–10 ng/mL	AFP, IgG, GPC3, HSA	Human serum	60	[125]
	Pt, Pd	RGO–CMCS–Hemin/PtNPs&PdNP/Apt_{GP73} CP: Apt_{A10-2}	Colorimetric	4.7 ng/mL	10–110 ng/mL	HSA, IgG, AFP	Human serum	120	[126]
	Au	SPCE/AuNPs/POPD/Apt_{A10-2}BSA Hemin–RGO–Mn_3O_4/Apt_{GP73}	SWV	0.0071 ng/mL	0.01–100.0 ng/mL	CEA, AFP, HSA, IgG	Human serum	60	[127]
	Au	SPCE/AuNPs/RGO-PANI@Fc/Apt_{GP73}/cDNA	DPV	0.15 pg/mL	0.001–100 ng/mL	AFP, BSA, HSA, IgG, LDL, ROS	Human serum	60	[128]
	Au, Cu	SPCE/AuNPs/Apt_{GP73}/BSA Hemin/Cu/MOF/Apt_{A10-2I}	DPV	0.625 ng/mL	1.0–300.0 ng/mL	IgG, IgE, AFP, HAS, BSA,	Human serum	120	[129]
Fucosylated–GP73	Au	AuE/Apt_{GP73}/MCH (CP) AuNPs/A–LCA/B–HRP (DP)	DPV	7 pg/mL	10 pg/mL – 25 ng/mL	AFP, BSA, non fucosylated-GP73	Human serum	40	[130]
GPC3	Au	SPCE/AuNPs/$Apt_{Ap613-1}$/BSA (CP) HGN/$Apt_{Ap613-1}$ (DP) + Ag^{+} in solution with H_2O_2	DPV	3.16 μg/mL	10–100 μg/mL	AFP, BSA, IgG, IgE, HSA	Human serum	150	[131]
		SPCE/AuNPs/RGO-Hemin/Apt $_{Ap613-1}$	DPV	2.86 ng/mL	0.001–10 μg/mL	BSA, IgE, IgG, HSA, AFP	Human serum	30	[132]
		$LAPS_{chip}$/APTES/AuNPs/PEI/RGO/$Apt_{Ap613-1}$	LAPS	40.0 ng/mL	0.1–100.0 μg/mL	$Apt_{GPC3-ROS,}$ IgG, IgE, HSA	Spiked serum samples	60	[133]
	Au, Fe_3O_4	CDs/AuNPs/Apt@Fe_3O_4/$GO_{nanosheets}$	FRET	3.01 ng/mL	5–100 ng/mL	HSA, AFP, IgG, IgE	Human serum	120	[134]

(*continued on next page*)

Table 3 (*continued*)

Target biomarker	Metalic nanoparticle	Platform	Detection method	LOD	Linear range	Selectivity studies	Real sample analysis	Incubation time (min)	Ref.
	Pt, Pd	SPCE/PtNPs&PdNPs@RGO-Cs-Fc/ $Apt_{Ap613-1}$	DPV	3.69 ng/mL	0.001–10 μg/mL	BSA, HSA, IgG, IgE	Human serum	20	[135]
	Pd, Au	SPCE/AuNPs/POPD/Apt $_{Ap613-1}$/BSA PrGO/Hemin/PdNPs/$Apt_{Ap613-1}$	DPV	0.13 pg/mL	0.001–10 ng/mL	AFP, IgG, IgE, HSA, LDL	Human serum	90	[136]
	Pd, Au	SPCE/AuNPs/RGO-CMCS-Hemin-PdNPs/ $Apt_{Ap613-1}$/BSA	DPV	1 ng/mL	1–100 ng/mL	AFP, BSA, HSA, IgE, IgG	Human serum		[137]
	Au, Cu	SPCE/AuNPs/RGO-$Cu_2O_{nanozyme}$/$Apt_{Ap613-1}$/BSA	DPV Chronoamperometry	0.064 ng/mL 0.0177 ng/mL	0.1–500 ng/mL 0.1–50 ng/mL	BSA, IgG, HSA, AFP	Human serum	45	[138]
HepG2 cell	Au, Pt	ITO/AuNPs/Apt_{TLS11a}/MCH PtNPs/$cDNA_1$-Fc/BSA PtNPs/$cDNA_2$-Fc/BSA	DPV	15 cells/mL	50–1 × 10^6 cell/mL	MCF-7 MDA-MB-231	–	90	[139]
HepG2–MVs	Au	GFET/RGO/AuNPs/Apt_{EpCAM}&Apt_{TLS11a}/MCH	Field–effect transistor	84 particles/μL	6 × 10^5–6 × 10^9 particles/mL	AFP, CEA	Human serum	30	[140]
SMMC–7721 exosome	Au	SPR_{AuChip}/AuNPs@PDA/cDNA-TPs/ $Apt_{SMMC-7721}$ AuNPs@PDA/Apt_{CD63}	SPR	5.6 × 10^5 particles/mL	–	Exosomes from HepG2, Bel-7404, L02, MCF-7, SW480	Human serum	100	[141]
SHh	Au	GCE/AuNPs/MCH/CP-S2-Biot Apt_{SHh},Strep-HRP, Exonuclease III in solution	Chronoamperometry	3.34 pM	0.005–1 nM	CEA, PDGF–BB, AFP	Diluted serum	60	[142]

sAuNPs - Spindle-shaped gold nanostructure; AA - Ascorbic acid; AFP - Alpha-fetoprotein; AgNPs - Silver nanoparticles; A-LCA – Avidin-lens culinaris agglutinin; Apt - Aptamer; APTES - 3-Aminopropyltriethoxysilane; ATP - Adenosine triphosphate; AuE - Gold electrode; AuNPs - Gold nanoparticles; Bel-7404 - Hepatocellular carcinoma cell line; B-HRP - Biotinylated horse radish peroxidase; BSA - Bovine serum albumin; CA - Cancer antigen; Cap - Capture; CD - circular dichroism; CD63 - Cell surface antigen; cDNA - Complementary DNA; CDs - Carbon dots; CEA - Carcinoembryonic antigen; CL - Control line; CMCS - carboxymethyl chitosan; Con - Control; CoP - Conjugate pod; CP – Capture probe; S2-Biot – Biotinylated S2 sequence; CS - Chitosan; Cy3 - Cyanine 3; Det - Detection; DP: detection probe; DPV - Differential pulse voltammetry; Fc - Ferrocene label; FRET - Fluorescence resonance energy transfer; FTOG - Fluor-doped tin oxide glass; GCE - Glass carbon electrode; GFET- Graphite field-effect transistor chip; GLU - Glucose; GO - Graphene oxide; GP73 - Golgi Protein 73; GPC3 - Glypican 3; HBsAg - Hepatitis B surface antigen; HCG - Human chorionic gonadotropin; HepG2 - Hepatocellular carcinoma cell line; HER2 - Human epidermal growth factor receptor 2; HGNs - Hemin graphene hybrid nanosheets; HSA - Human serum albumin; ITO - Indium tin oxide; L02 - Human fetal hepatocyte line; LAPS -Light-addressable potentiometric sensor; LDL - Low density lipoprotein; LFD: lateral flow device; LOD - Limit of detection; MBIA - 2-mercaptobenzimidazole-5-carboxylic acid; MCF-7 - breast cancer cell line (ER+, HER-); MCF-7 - Breast cancer cell line (ER+, HER-); MCH - 6-Mercapto-1-hexanol; MDA-MB-231 - breast cancer cell line (ER-, HER-); MOF - metal-organic framework; MPTES - 3-Mercaptopropyltriethoxysilane; Mtase - Methyltransferase; MUC1 - Mucin 1; NA - Not available; N-Cn-box - Nitrogen doped carbon nanoboxes; NE - Norepinephrine; N-GQDs - Nitrogen dopen graphene quantum dots; $Ni(OH)_2$ - Nickel(II) hydroxide; PANI- Polyaniline; PDA – Polydopamine; PDGF-BB - Platelet growth factor; PdNPs - Palladium nanoparticles; PEC – Photoelectrochemical; PEI - Polyetherimide; PET - Photoinduced electron transfer; POPD - Poly(o-phenylenediamine); PrGO - Phosphorus doped reduced graphene; PSA - Prostate-specific antigen; PTK7 - Protein tyrosine kinase 7; PtNPs - Platinum nanoparticles; QD - Quantum dots; RCDs - Red carbon dots; RGO - Reduced graphene oxide; ROS - Random ssDNA sequence; SERS - Surface-enhanced Raman scattering; SHh - Sonic Hedgehog; SMMC-7721 - Hepatic carcinoma cells; SPCE - Screen printed carbon electrode; Strep-HRP -Streptavidin horseradish peroxide conjugate; SW480 - Colon adenocarcinoma cell line; SWV - Square wave voltammetry; Tel - Telomerase; TH - Thionin; THR - Thrombin; TL - Test line; TPs - Tetrahedron probes; TYR - Tyrosine; UCNP - Upconversion nanoparticles; VEGF - Vascular endothelial growth factor; Vit - Vitamin.

assembly of DNA-modified AuNP dimers with strong chiroptical activity. Upon AFP binding, the aptamer-DNA duplex is disrupted, reducing the circular dichroism intensity and enabling detection in the nM range [110]. Fluorescence resonance energy transfer (FRET) was used to detect AFP with an aptamer-labeled with CdTe QDs acting as the donor and an anti-AFP antibody-AuNP as the acceptor. The biomolecular interactions between the aptamer, target and antibody brought the QDs and AuNPs into proximity, leading to quenching of CdTe QDs emission. This signal-off aptasensor reaches a LOD of 400 pg/mL [111]. PdNPs can quench the fluorescent emission of 5-carboxyfluorescein (FAM) through interaction with aptamer nitrogen functional groups, but the AFP concentration range is one order of magnitude higher [115]. Lateral flow devices (LFD) are very appealing for their simple handling, visual detection and quickness, in qualitative analysis. However, even when using a portable strip reader in the test zone the detectability is significantly poorer than FRET though the procedure is much faster [112]. This LFD is a sandwich assay using a unique aptamer sequence, indicating that AFP has at least two distinct binding sites for it. PtNPs [114] or hybrid Au-PtNPs [113] combined with other graphene-based nanostructures on SPCE achieved the detection of low AFP concentrations (ng/mL) even in a reagentless format [113]. While most approaches discussed required a 60 min incubation time [108–110,113], the FRET-based sensor required up to 80 min [111] and LFD just 10 min.

Several other types of NPs have been explored for AFP sensing. Rahmati *et al.* developed an SPCE aptasensor modified with hierarchical porous $Ni(OH)_2$ nanosheets on hollow N-doped carbon nanoboxes. By electrochemical impedance spectroscopy (EIS) fM to nM sensitivity was achieved [116]. An innovative approach employed red carbon dots (RCDs) from blood orange, which adsorbed AFP aptamer via π-π stacking, leading to fluorescence quenching through a photoinduced electron transfer effect. Upon AFP binding, the aptamer detached from the RCD surface, restoring fluorescence. This method was also applied for AFP imaging in HCC cells [117]. CDs enhanced photoelectrochemical biosensor activity of TiO_2 and In_2S_3, achieving a LOD in the low pM range [118]. Surface-enhanced Raman scattering (SERS) provides exceptional optical enhancement for AFP detection due to its narrow spectral peaks and high specificity. Two SERS-based biosensors were developed, both achieving a linear detection range down to aM. In the first approach, silver NPs trimers (Ag-trimers) were formed by hybridization between two ssDNA and the aptamer. AFP binding disrupted the Ag-trimer structure, leading to SERS signal off measurements [119]. In the second strategy, Qu *et al.* developed an aptamer-based biosensor using AuNPs and up-conversion nanoparticle trimers for simultaneous AFP and mucin-1 (MUC1) detection. The SERS intensity decreased in the presence of MUC1, while luminescence intensity increased in the presence of AFP [121]. Even though dual-target detection is an obvious advantage, the incubation time with the two proteins was 600 min [121], compared to just 30 min in the first SERS example discussed [119]. Another SERS sensor recently developed utilizes a Au@Janus@AgNP platform functionalized with cyanine 3 (Cy3) and 2-mercaptobenzimidazole-5-carboxylic acid (MBIA). While its LOD was not as high as previously discussed sensors, its novelty lies in its signal-switching mechanism, where AFP binding triggered the release of one of the Raman signaling molecules (Cy3), thereby altering the SERS response, which is referred to the unaltered signal of MBIA used as internal calibration to correct experimental variations [120].

5.2. Sensing platforms for detecting GP-73

Even though GP-73 is not commonly used in daily clinical practice, interest in developing sensors for this biomarker remains high due to its improved sensitivity and specificity compared to AFP. Several innovative sensing strategies have been developed, incorporating nanomaterials such graphene quantum dots (GQDs), molybdenum disulfide (MoS_2), and metal-organic frameworks (MOFs). FRET mechanism allowed for highly sensitive GP-73 detection. Two aptasensors used nitrogen-doped graphene quantum dots (N-GQDs) as both the aptamer support and the emitter, and MoS_2 nanosheets with or without RGO, as a quencher. Both exhibited linear detection ranges in the low nM domain [122,123], but the first one has the advantage of increasing signals [123]. Similarly, MoS_2 was combined with Fc and PdNPs acting as both a fluorescence quencher and an electroactive molecule in a dual-mode detection. The LOD was significantly improved for fluorescence, but electrochemical detection was even more sensitive [125]. These aptasensors use a short aptamer that is referred to a SELEX from which that sequence was not selected. Importantly, we found this sequence as a MUC1 aptamer selected 20 years ago [143] and also used in the multiplex AFP-MUC1 aptasensor [121] (see Table 3). The same group developed several sandwich-type electrochemical aptasensors that required the attachment of that aptamer to different nanostructures carrying electroactive molecules [124] or with peroxidase activity through the presence of hemin that catalyzes the oxidation of 3,3′,5,5′-tetramethylbenzidine (TMB) [126,127]. A10-2 aptamer was used as the capture receptor on a centrifuge tube [126] or attached to Au nanostructures [124,127]. The use of TMB as the substrate of the nanozyme allows both colorimetric [126] and electrochemical detection [127]. In the latter case, the redox activity of hemin is also measured but the sensitivity is lower than the one provided by the TMB cathodic current. The ratiometric signal arisen from the Cu-MOF and the hemin [129] could not rival the detectability of the nanozyme approaches nor the competitive assay based on complementary strand displacement that reaches a LOD of 0.15 pg/mL [128]. The detection of specific glycoforms of a biomarker can be advantageous over the total protein content. An amperometric aptasensor was reported to detect the fucosylated GP-73, a potential biomarker to distinguish HCC from other liver diseases. The aptamer was used as the capture probe while a lectin-avidin conjugate immobilized on AuNPs recognized the fucose moiety. The AuNPs provided a large immobilization area for the lectin, allowing for a high loading capacity of biotinylated horseradish peroxidase (HRP) via avidin-biotin interactions [130].

5.3. Sensing platforms for detecting GPC3

Another biomarker that has gained increasing interest in recent years is GPC3, with the first aptasensing publication appearing in 2020 and research in this field steadily expanding. The first GPC3 electrochemical aptasensor utilized hemin/graphene nanohybrids (HGNs) to catalyze peroxidase-like silver deposition in the presence of H_2O_2. The Ap613-1 aptamer was immobilized by adsorption on graphene. The same aptamer was also immobilized on AuNPs probably through chemisorption to capture GPC3, though the thiol group is not explicitly indicated. The sandwich format suggests the presence of two identical binding sites for the same aptamer on GPC3. However, the LOD of 3.16 μg/mL is not impressive [131]. Thus motivated, the replacement of GO by RGO and the covalent attachment of the aptamer significantly improved the sensitivity by three orders of magnitude. The storage stability was marginally improved [132]. The use of a Si-based LAPS chip coated with RGO/polyetherimide/AuNPs yielded a less sensitive approach [133].

For fluorescence-based detection, a FRET aptasensor was developed using GPC3 aptamer-functionalized gold carbon dots (AuCDs) as the donor and magnetic GO nanosheets (Fe_3O_4/GO) as the acceptor [134]. However, the aptamer used is traced to a SELEX where this sequence is not reported. We have found this sequence used to recognize the platelet-derived growth factor [144]. Several electrochemical aptasensors for GPC3 have been designed by combining different NPs (Au, Pt, Pd, Cu) with nanomaterials. They have catalytic activity or carry electroactive species [135–138]. Those approaches are similar to those described for GP73 detection. The most sensitive transduction technique was chronoamperometry that reaches pg/mL level when measuring the catalytic activity of the Cu-based nanozyme [138].

5.4. Sensing platforms for detecting other targets

AuNPs have been widely utilized in the design of sensing platforms for the detection of HCC-related targets such as cells [139], microvesicles (MVs) [140], and exosomes [141]. In one study, HepG2 cells were detected on ITO electrodes modified with TLS11a aptamer chemisorbed onto AuNPs in a strand displacement assay. The detection probe is a crosslinked structure of Fc-cDNA sequences immobilized onto PtNPs. The initial Fc current is very high and decreases when the target cells bind displacing the nanoparticle mesh. The sensing layer is regenerable by removing all the structures anchored on AuNPs applying pulses at high negative potentials. This method required a 90 min incubation time [139]. For HepG2 MVs, a dual-aptamer modified RGO field-effect transistor nanosensor was developed, incorporating an epithelial cell adhesion molecule (EpCAM) aptamer as part of the sensing platform. EpCAM is a common surface protein used to isolate any type of vesicles, so the selectivity is provided by the cell-specific aptamer. This approach reduced the required incubation time by two-thirds compared to the previous method [140]. In another study, Liao *et al.* used SPR, a technique less commonly employed in HCC aptasensing. Their platform featured a dual-aptamer system targeting exosomes derived from hepatic carcinoma SMMC-7721 and CD63 as a commonly expressed protein on vesicle surfaces [141]. We were unable to trace the original SELEX of this specific aptamer ZY-sls. It was used hybridized on a DNA tetrahedron structure to reduce the unspecific binding in comparison with binary SAMs. The SPR signal was double amplified due to the secondary anti-CD63 aptamer on an Au nanostructure and the subsequent deposition of Au. The Sonic Hedgehog (SHh) signaling pathway is closely associated with cancer metastasis, drug resistance, and poor HCC prognosis. To address this, an electrochemical aptasensor based on exonuclease III activity that can cleave dsDNA was designed. The aptamer has a hairpin structure to be cleaved. The cleaved aptamer can replace a biotinylated probe hybridized on the electrode. Subsequent streptavidin-HRP binding catalyzes TMB/H_2O_2, reaction. In the presence of the target, the SHh/aptamer complex formed inhibits the cleavage, retaining the biotinylated probe, so increasing the TMB reduction current, and allowing for SHh detection down to 3.34 pM [142].

Selectivity studies were conducted to demonstrate the specific behavior of the developed aptasensors in more complex media. These studies typically involved common serum proteins, like bovine and human serum albumins, immunoglobulin G and E, thrombin or even AFP, ensuring robustness in real-world applications.

It is worth noting the use of sequences that cannot be traced to a SELEX to select the intended target. Moreover, those sequences are reported for recognizing other molecules. This highlights the importance of carefully selecting aptamers from the literature and accurately referencing the original SELEX study in subsequent research to ensure proper performance and reproducibility.

Some of the most innovative sensing strategies targeting HCC-related biomarkers are illustrated in Fig. 4.

6. Applications of aptamers in cancer therapy

Despite advancements in biomarker discovery and screening strategies, HCC is still frequently diagnosed at advanced stages, leaving systemic therapy as the primary treatment option for many patients [145]. Developing highly effective therapeutics for HCC is a burdensome challenge because of the poor penetration of chemotherapeutic agents into the tumor site, chemoresistance, and severe toxicity to healthy tissues, which significantly undermines therapeutic outcomes [146, 147]. Aptamer-mediated nanotechnology is a powerful tool for the

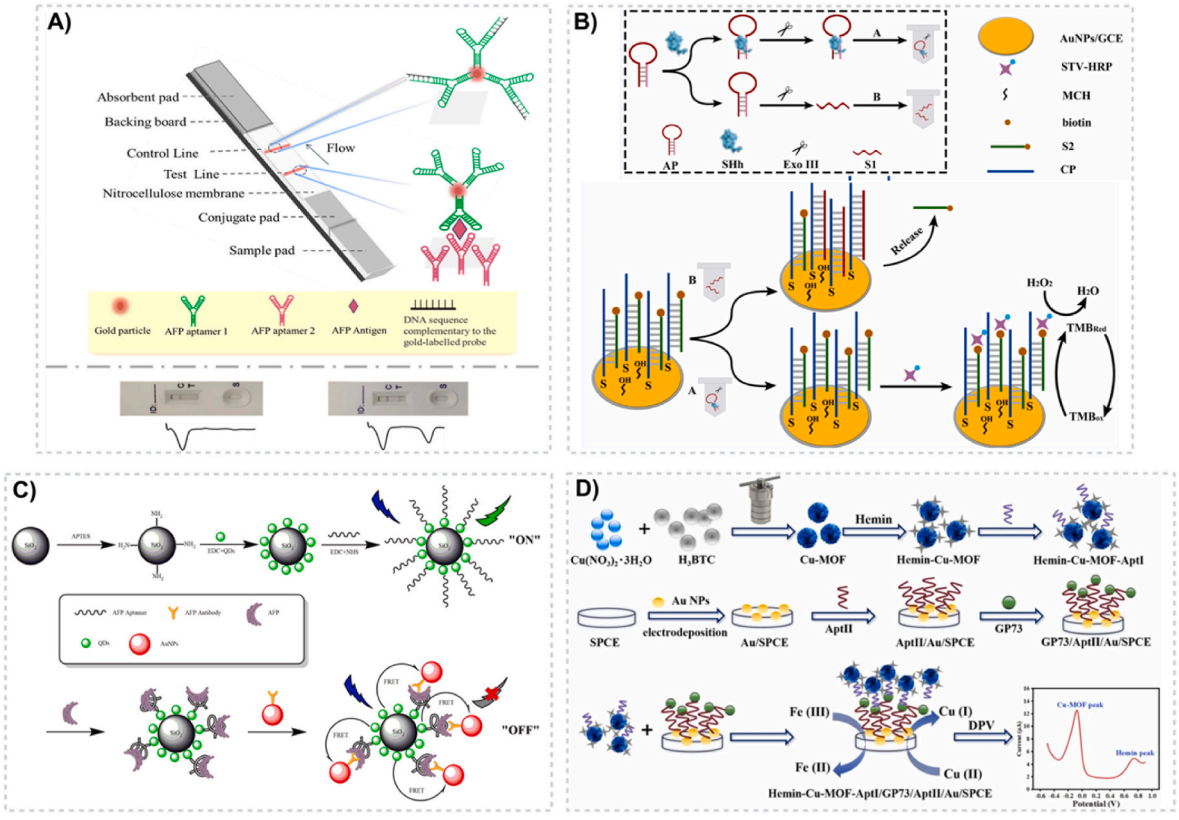

Fig. 4. Aptamer-based sensing platforms for HCC biomarker detection. Schematic representation of **A)** lateral flow colorimetric aptasensor for AFP detection (reprinted from open access Ref. [112]); **B)** target-induced enzyme activity inhibition based electrochemical aptasensor for SHh detection (reprinted with permission from Ref. [142]); **C)** fluorescent sandwich aptasensor for AFP detection (reprinted with permission from Ref. [111]); **D)** dual-signal ratiometric electrochemical aptasensor for GP-73 detection (reprinted with permission from Ref. [129]).

targeted delivery of chemotherapeutics, combining the advantages of nanotherapeutics, such as improved physicochemical and pharmacokinetic properties of antitumor drugs [148], with the high specificity of aptamer-target interactions, thereby minimizing off-target toxicity [149]. Herein, we discuss some of the most significant aptamer- and nanoparticle-based active targeting strategies for the delivery of chemotherapeutics for the treatment of HCC, highlighting the advantages and limitations of aptamer-based active targeting. The examples discussed are summarized in Table 4 and Appendix C, which contain detailed information regarding the specific aptamer sequence used in each study, type of nanocarrier, platform design, incorporated drug, and the types of cells tested.

6.1. Nucleolin targeting strategies

AS1411 is a guanosine-rich DNA aptamer that binds nucleolin and was discovered by Bates *et al.* [176]. It exhibits antiproliferative properties in HCC by modulating galectin-14 expression [177]. G-quadruplex structured aptamers as AS1411 offer advantages such as increased stability, resistance to nuclease digestion, non-immunogenicity, and enhanced cellular uptake, making them suitable for *in vivo* therapeutic applications [176,178]. This oligonucleotide has been extensively explored in different drug delivery systems for HCC targeted therapy [150–155] and theranostics [156,157].

Huang *et al.* utilized AS1411 aptamer for active targeting in a simple phyto-chemotherapeutic strategy for HCC. They developed biodegradable and biocompatible poly lactic-co-glycolic (PLGA) NPs loaded with polyphyllin II (PPII), a steroidal saponin [150]. This approach improved the water solubility of PPII and enhanced the cellular uptake in nucleolin-positive cells, effectively inducing cell apoptosis. Building on this, a dual antitumor targeted therapy system was developed by incorporating a photosensitizer (IR780) for photothermal therapy [151]. The functionalized NPs exhibited a dual pH and NIR response, facilitating controlled drug release at the tumor site, both *in vitro* and *in vivo*.

To prolong the systemic circulation time of aptamer-nanoconjugates, Abd-Rabou *et al.* developed a PEGylated NP system with chemically modified AS1411 for the actively targeted delivery of viramidine (VIR), a prodrug of ribavirin acting as a nucleoside inhibitor with potential anti-HCC therapy. The modified ribose backbone of AS1411 aptamer demonstrated a 2.5-fold increased affinity for nucleolin-expressing HCC cells compared to that of unmodified aptamer [152]. The chemical modification started from the premise that normally the aptamer backbone is very flexible, thus making target-induced adaptive folding more difficult. Consequently, the thymidines at positions 1–12 were randomly substituted with 5-(N-benzylcarboxyamide)-2′-deoxyuridine, resulting in a modified AS1411 aptamer with stronger stability and enhanced affinity towards nucleolin [179]. This modified AS1411 aptamer, in combination with PEGylated nanocarriers, has been explored in other active targeted delivery formulations, such as nanoliposomes or poly(lactic acid) micelles for the delivery of apigenin [153] or the co-delivery of doxorubicin (DOX) and miR-519c [154], with promising *in vivo* results for HCC treatment. DOX is a highly effective chemotherapeutic agent due to its ability to intercalate DNA and inhibit cell proliferation [180]. Inspired by this mechanism, Trinh *et at.* developed a synthetic DOX-AS1411 aptamer adduct as a novel therapeutic approach for HCC, based on the recognition capability of AS1411 aptamer and the antitumor efficacy of DOX [155]. Moreover, the adduct protected the DNA backbone from nuclease digestion, improving the pharmacokinetic properties of the aptamer.

Theranostic strategies, which integrate imaging, diagnostics, and therapy, are gaining attention in cancer research [156]. Zhao *et al.* developed a small interfering RNA (siRNA) delivery vector combining the excellent properties of carbon quantum dots (CQD) for *in vivo* applications, with the gene silencing ability of siRNA and the targeting capability of AS1411 aptamer to enable both bioimaging and targeted gene therapy for inhibiting HCC metastasis [157]. This method addresses the drawbacks of traditional viral and non-viral vectors, including immunogenicity, cytotoxicity of transfection agents and inability to protect the miRNA from nuclease digestion, providing a more biocompatible and environmentally friendly alternative for HCC theranostics. Another theranostic strategy consisted in the use of CS as the nanocarrier, a positively charged linear polysaccharide characterized by easy penetration through cell membranes and pH-responsiveness [181]. CS was combined with gold nanoclusters for methotrexate (MTX) encapsulation [156]. This strategy not only mitigated the systemic toxicity of MTX but also presented low cytotoxicity, pH-dependent controlled release, and high fluorescence efficiency, enabling bio-tracking through Au nanoclusters.

6.2. HCC cell targeting strategies

TLS11a is an extensively explored DNA aptamer in HCC therapy, owing to its strong binding affinity towards HCC (MEAR) cells [79]. Over the years, various targeting strategies have been developed using this aptamer, ranging from conventional active delivery of chemotherapeutics [158] to multimodal approaches that integrate chemotherapy with photothermal (PTT) [159] and photodynamic (PDT) therapies [160,161]. These strategies also show innovation through the diverse nanocarriers exploited, including MSiNPs, AuNPs, Fe_3O_4, BPQDs.

Ding *et al.* developed a dual-targeting system by conjugating liposomes on MSiNPs, enabling efficient recognition of both liver cancer cells and their nuclei *in vivo*. This system used TLS11a aptamer and TAT peptide as the recognition elements [158]. The TAT peptide binds to the nuclear pore complex, preventing the activation of the multi-drug resistance mechanism and facilitating the direct transport of DOX into the nuclei.

PTT is frequently combined with targeted treatment strategies because of the ineffectiveness of single treatment modalities and the spatial selectivity of photosensitizers for laser irradiation [182]. To overcome the poor pharmacokinetic properties of chlorine e6 (Ce6), an FDA approved traditional photosensitizer [183], Zhang *et al.* conjugated Ce6 to the 5′ end of TLS11a aptamer and modified the 3’ end with $(GA)_{10}$ repeating nucleotides to serve as a carrier for AQ4N (a topoisomerase II prodrug) *via* Cu(II) complexation [160]. This host-metal-guest architecture was grafted onto AuNPs to obtain a smart pH-responsive platform capable of synergistic photothermal, photodynamic, and chemotherapeutic effects *in vivo*. Recent studies focused on replacing traditional photosensitizers with less toxic and more biodegradable compounds such as GQD [184,185]. Chen *et al.* developed a synergistic photothermal-chemotherapeutic system, consisting of Fe_3O_4 NPs coated with CS [159]. TLS11a aptamer, DOX and GQD were grafted onto these nanoparticles. Compared to the previously mentioned strategy, both approaches employed passive (pH-responsive) and active (aptamer-based) targeting *in vitro* and *in vivo*, but the use of GQD instead of Ce6 reduced toxicity. Another PDT example consisted of using BPQDs, which can generate reactive oxygen species, combined with PtNPs to enhance PDT through a self-compensation mechanism. This approach transformed H_2O_2 into O_2, counteracting the hypoxic tumor microenvironment [161]. Interestingly, the same Cell-SELEX process [79] yielded multiple aptamer sequences that have been explored for active targeted therapy in HCC. Chakraborty *et al.* investigated the recognition ability of phosphorothioate backbone-modified TLS9a aptamer compared to various cell-targeting ligands, further expanding the potential of aptamer-based therapies for HCC treatment [162].

6.3. EpCAM targeting strategies

EpCAM targeting aptamers have been thoroughly explored in HCC for theranostic approaches [163–165], gene [166] and gene-chemotherapy [166–169], due to the immunogenic properties of this transmembrane glycoprotein. Targeted therapy strategies have

Table 4
Aptamer based targeted therapy strategies for HCC reported in the literature.

Target biomarker	Aptamer	Application	Nanocarrier	Platform design	Incorporated drug	Encapsulation efficiency (%)	Drug loading efficiency (%)	Type of cells used	*In vitro/ in vivo*	Ref.
Nucleolin	AS1411	Targeted therapy	PLGA-NPs	PLGA-NPs@PPII/Apt	PPII	80.98 ± 1.63	7.29 ± 0.08	HepG2	*Both*	[150]
			PLGA-NPs	PLGA-NPs/IR780/ PPII/Apt	PPII IR780	–	3.77 ± 0.05 2.95 ± 0.02	HepG2	*Both*	[151]
			PEG-PLGA-NPs	PEG-PLGA-NPs/ VIR@Apt	VIR	86.9 ± 6.7	–	HepG2 Huh-7	*In vitro*	[152]
			PEG-NLs	PEG-NLs@Api/Apt	API	86.6 %	4.33 ± 0.05	HepG2 Huh-7	*Both*	[153]
			PEG-PLA-MC	PEG-PLA-MC/miR-519c/Apt	DOX miR-519c	51.93 86.53	4.76 0.68	HepG2	*Both*	[154]
			–	Apt-DOX	DOX	–	–	Hu767	*Both*	[155]
		Theranostic	CS-AuNCs	CS-AuNCs@MTX/Apt	MTX	–	14.2	HepG2	*In vitro*	[156]
			CDs	CDs/Cy3-Apt/Cy5-siRNA	siRNA	–	–	HepG2	*In vitro*	[157]
MEAR cell line	TLS11a	Targeted therapy	MSiNPs	MSiNPs-TATp@LB@DOX/Apt	DOX	83.33 %	–	H22	*Both*	[158]
		Targeted therapy PTT	Fe_3O_4@CS-NPs	Fe_3O_4@CS-NPs@DOX/GQD/Apt	DOX	85 %	12 %	H22	*Both*	[159]
		Targeted therapy PTT PDT	AuNPs	AuNPs/Apt-Ce6/ Cu^{+2}-AQ4N	AQ4N	53.01	–	HepG2	*Both*	[160]
		PDT	MSiF@BPQDs&PtNPs	MSiF@BPQD&PNPst/ Apt	–	–	–	HepG2	*Both*	[161]
TAG-72 HSP70	TLS9a	Therapy	PLGA	PLGA-NPs@PTX/Apt	PTX	70.95 ± 3.69	6.45 ± 0.45	HepG2 Huh-7	*Both*	[162]
EPCAM	EpCAM-Apt-1	Theranostic	Fe_3O_4@CMC-NPs	Fe_3O_4@CMC-NPs@DOX/Apt	DOX	98	24	HepG2	*In vitro*	[163]
	EpCAM-Apt-2		USI-NPs (nanocarrier-free approach)	USI-NPs/LMWP@UA-SRF/Apt	SRF UA	–	–	HepG2 H22	*Both*	[164]
	EpCAM-Apt-3		MSiNPs	MSiNPs-PEG@5-FU@AuNPs/Apt	5-FU	31.33 % ± 1.41	23.87 % ± 0.82	HepG2	*Both*	[165]
	EpDT3	Gene therapy	Ad5	Ad5-PTEN/PEG/Apt	PTEN	–	–	HepG2	*Both*	[166]
	EpCAM-Apt-4	Chemo- and gene therapy	CyD-PRNSs	CyD-PRS-Apt-siRNA @SRF	SRF	–	–		*Both*	[167]
	EP166		NPC (Pharmacosome)	$NPC_{(@5'\text{-}DFUR)}$/ miRNA-122/Apt	5′-DFUR miRNA-122	–	–	HCCLM3	*In vitro*	[168]
	EpCAM-Apt-5		h-MSiNPs	h-MSiNPs/CRISPR-Cas9 system/Apt-PAMAM	SRF CRISPR-Cas9	78.25 76.65	23.15 –	HepG2	*Both*	[169]
Glypican 3	AP613-1	Imaging	USPIO	USPIO/Apt	–	–	–	Huh-7	*Both*	[170]
		Theranostic	h-MnO_2	h-MnO_2–PEG@SRF/ Apt	SRF	–	–	Huh–7 HepG2	*Both*	[171]
CD133	A15	Targeted therapy	NLs	NLs@XAV-939/ DOX@Apt/ UAMC1110	DOX XAV-939	96.351 ± 0.877	1.950 ± 0.018	Hepa1-6	*Both*	[172]
						78.509 ± 4.372	0.230 ± 0.013			
			SLNPs	SLNPs/PEG/OXA/A54 SLNPs/PEG/SAL/Apt	OXA SAL	65.3 ± 1.9 84.42 ± 0.55	3.46 ± 0.12 7.77 ± 0.28	CD133+	*Both*	[173]
CD133 EGFR	A15 CL4	Therapy	PLGA-PEG	PLGA-PEG@SAL/ Apt_{A15}&Apt_{CL4}	SAL	58.1 ± 7.3	7.0 ± 0.6	Huh-7 Hep3B	*In vitro*	[174]
Carbohydrate sialyl Lewis X	sLeX-AP	Therapy	CNTs	CNTs/PEI@DUmab/ Apt-siRNA chimera	DUmab siRNA	–	–	HepG2	*Both*	[175]

5′-DFUR - Doxifluridine; 5-FU - 5-Fluorouracil; A54 - HCC specific peptide; Ad5 - Recombinant adenovirus type 5; API - Apigenin; AQ4N - Banoxantrone; AuNCs - Gold nanoclusters; BPQDs - Black phosphorus quantum dots; CDs - Carbon dots; CD133 - Prominin I antigen; Ce6 - Chlorine e6; CMC - Carboxymethyl cellulose; CNTS - Carbon nanotubes; CQD - Carbon quantum dots; CS - Chitosan; Cy3 - Cyanine 3 orange fluorescent dye; Cy5 - Cyanine 5 red fluorescent dye; CyD-PRNSs - Cyclodextrin porous RNA nanospheres; DOX - Doxorubicin; DUmab - Durvalumab; EGFR - Epidermal growth factor receptor; EPCAM - Epithelial cell adhesion molecule; GQD - Graphene quantum dots; H22 - Mouse hepatocellular carcinoma cell line; HCCLM3 - Hepatocellular carcinoma cell line with high metastatic potential; Hep3B - Hepatocellular carcinoma cell line; Hepa1-6 - Mouse hepatocellular carcinoma cell lines; HepG2 - Human hepatocellular carcinoma cell line; h-MnO_2 - Hollow manganese oxide; h-MSiNPs - Hollow mesoporous silica nanoparticles; HSP70 - Heat shock protein 70; Hu767 - Human primary hepatocytes; Huh7 - Human hepatocellular carcinoma cell line (glypican3 positive); IR780 - Heptamethine cyanine NIR fluorescent probe; LB - Lipid bilayer; LMWP - Low molecular weight protamine; MC - Micelles; miR-519c - Small non-coding RNA; MSiF - Mesoporous silica framework; MSiNPs - Mesoporous silica nanoparticles; MTX - Methotrexate; NLs -

Nanoliposomes; NPC - O,O'-((2R,3R,4R,5R)-2-(5-fluoro-2,4-dioxo-3,4-dihydropyrimidin-1(2H)-yl)-5-methyltetrahydrofuran-3,4-diyl) dioctadecyl dioxalate; OXA - Oxaliplatin; PAMAM - Poly(amidoamine); PDT - Photodynamic therapy; PEG - Polyethylene glycol; PEI - Polyethyleneimine; PLA - Polylactic acid; PLGA - Poly(lactic-co-glycolic acid); PPII - Polyphyllin II; PTEN - Phosphate and tension homolog tumor suppressor gene; PTT - Photothermal therapy; PTX - Paclitaxel; SAL - Salinomycin; siRNA - Small interfering RNA; SLNPs - Solid lipid nanoparticles; SRF - Sorafenib; TAG-72 - Tumor-associated glycoprotein 72; TATp - Nuclear localization signaling peptide; UA - Ursolic acid; USI-NPs - Sorafenib, ursolic acid, and indocyanine green condensed nanoparticles; USPIO - Ultrasmall superparamagnetic iron oxide; VIR - Viramidine.

demonstrated innovation through a broad range of antitumor mechanisms, including the use of recombinant adenoviruses engineered to deliver tumor suppressor genes [166], pharmacosomes derived from doxifluoridine incorporating DNA encoding miR-122 [168], co-delivery systems combining CRISPR/Cas9 gene therapy and TKI (SRF) [169] and RNA porous nanospheres containing both EpCAM aptamers and siRNA designed as nanocarriers for SRF [167].

Theranostic strategies employing EpCAM-targeting aptamers have been successfully implemented in HCC for tumor visualization and drug delivery. Examples include MRI-based imaging using carboxymethylcellulose-coated Fe_3O_4 magnetic NPs loaded with DOX [163] and enhanced contrast in X-ray-based computer tomography based on the hybridization of AuNPs on PEG-ylated mesoporous silica NPs doped with 5-fluorouracil [165]. Le *et al.* explored the self-assembly properties of ursolic acid, a pentacyclic triterpenoid with antitumor properties, to develop a drug nanoskeleton loaded with SRF and indocyanine green [164]. This nanosystem facilitated imaging and dual-targeting HCC cells, through EpCAM aptamer and a tumor-penetrating peptide.

6.4. GPC3 targeting strategies

MRI-based imaging of HCC tumors has been further explored by targeting highly specific biomarkers such as GPC3 [170,171]. Initially, a simple imaging approach was developed using aptamer AP613-1 decorated ultrasmall superparamagnetic Fe_3O_4 [170]. Building on this, Wang *et al.* later designed a smart multifunctional strategy for both imaging and therapy using hollow mesoporous MnO_2 NPs for SRF delivery [171]. Upon aptamer-GPC3 binding, the nanoplatform released SRF at the tumor site, triggering pH-induced degradation of the MnO_2 NPs and released Mn^{2+} into the tumor microenvironment, thus enhancing MRI contrast and improving imaging precision.

6.5. Liver cancer stem cells targeting strategies

Tumor growth, metastasis and recurrence following initial successful therapy are often associated with the presence of liver cancer stem cells (LCSCs) [186]. Prominin-1 (CD133) is one of the most extensively characterized biomarkers for LCSCs, making it a promising target for active drug delivery [187]. Several targeted delivery strategies have been developed using CD133-specific aptamer (A15), including the delivery of salinomycin [174] and sequential therapy with salinomycin and oxaliplatin [173].

In HCC, resistance to conventional therapy often arises due to the protective role of cancer-associated fibroblasts (CAFs), which form a barrier on the surface of LCSCs, thus hindering drug delivery. To overcome this challenge, Kong *et al.* developed a multifunctional nanoliposome capable of targeting both CAFs and LCSCs [172]. The nanoliposome was fabricated to first target fibroblast-activating protein (FAP) on the surface of CAFs with FAP-inhibitor UAMC1110, thus activating barrier disruption and enabling penetration. Subsequently, the targeting of LCSCs was achieved *via* an aptamer specific to CD133. This dual-targeting strategy enabled efficient delivery of DOX and XAV-939, a Wnt/β-catenin signaling inhibitor, demonstrating significant antitumor efficacy both *in vitro* and *in vivo*. These results highlight the potential of such strategies in overcoming therapeutic resistance and the recurrence of HCC in treated patients.

6.6. Other targeting strategies

Current advancements in immunotherapy and its combination with other antitumor mechanisms have significantly improved survival rates in patients with advanced stage cancers, offering new treatment options for unresectable tumors [188]. Triggering receptor expressed on myeloid cells-2 (Trem-2) is a transmembrane receptor that regulates tumor immune response and contributes to the formation of immunosuppressive microenvironment, thus being a potential target to enhance the efficacy of immunotherapy in advanced HCC. Qiang *et al.* explored the inhibition of Trem-2 receptor through an siRNA-aptamer chimera, providing a new therapeutic approach for enhanced delivery of durvalumab [175].

As a summary, Fig. 5 highlights some of the most innovative aptamer-based targeted therapy strategies for HCC.

7. Application in clinical samples: challenges and perspectives

Since 1997, more than fifty antibody-based therapeutics for oncology have been approved by the FDA and EMA [189], with recent additions including gemtuzumab ozogamicin for acute myelogenous leukemia, trastuzumab emtansine for HER2-positive breast cancer and tisotumab vedotin for cervical cancer [44], highlighting the growing interest in targeted therapies. However, monoclonal antibodies, due to their large molecular weight (~150 kDa) and the binding site barrier effect, often exhibit limited tissue penetration. Their production via hybridoma technology is time-consuming (~6 months), costly and may induce immunogenic responses unless fully humanized or engineered as chimeric proteins [44]. To address these limitations, aptamers emerge as a viable substitute. Their compact size enables deeper tissue penetration and access to hidden epitopes that antibodies may not reach. In a study comparing an EpCAM-targeting aptamer with an antibody in tumor models, the aptamer demonstrated superior tumor core penetration, faster uptake (peak at 10 min), and longer retention (up to 26 h with PEGylation) compared to the antibody (peak at 3 h). Tumor accumulation was 1.67-fold and 6.6-fold higher for the aptamer at 3 and 24 h after intravenous administration, respectively [10].

The expiration of initial SELEX patents has made molecular affinity more accessible, driving a surge in start-ups and academic research dedicated to aptamer development and applications [190]. However, despite their potential, most aptamers have failed to meet the required safety and efficacy standards in human clinical trials [43,190]. This is due to various challenges discussed in previous sections, such as rapid degradation and renal clearance, which limit their effectiveness. For a long time, pegaptanib (Macugen) was the only aptamer used in clinical practice. Approved by the FDA in 2004 for treating age-related macular degeneration, it works by inhibiting blood vessel development through targeting the glycosylated homodimeric vascular endothelial growth factor (VEGF) isoform VEGF165. However, pegaptanib failed in the post-marketing stage due to the emergence of more effective alternatives like bevacizumab and ranibizumab, that generally target VEGF [191]. In August 2023, FDA approved avacincaptad pegol, the second-ever aptamer, for treating geographic atrophy, a leading cause of central vision loss with no cure. Until recently, no treatments were available, significantly affecting patients' quality of life. Its mechanism involves blocking the C5 protein to prevent immune attacks on retinal cells [192].

Although no aptamer-based cancer therapy is currently approved, AS1411 was the first to enter clinical trials. Its unique structure reduces

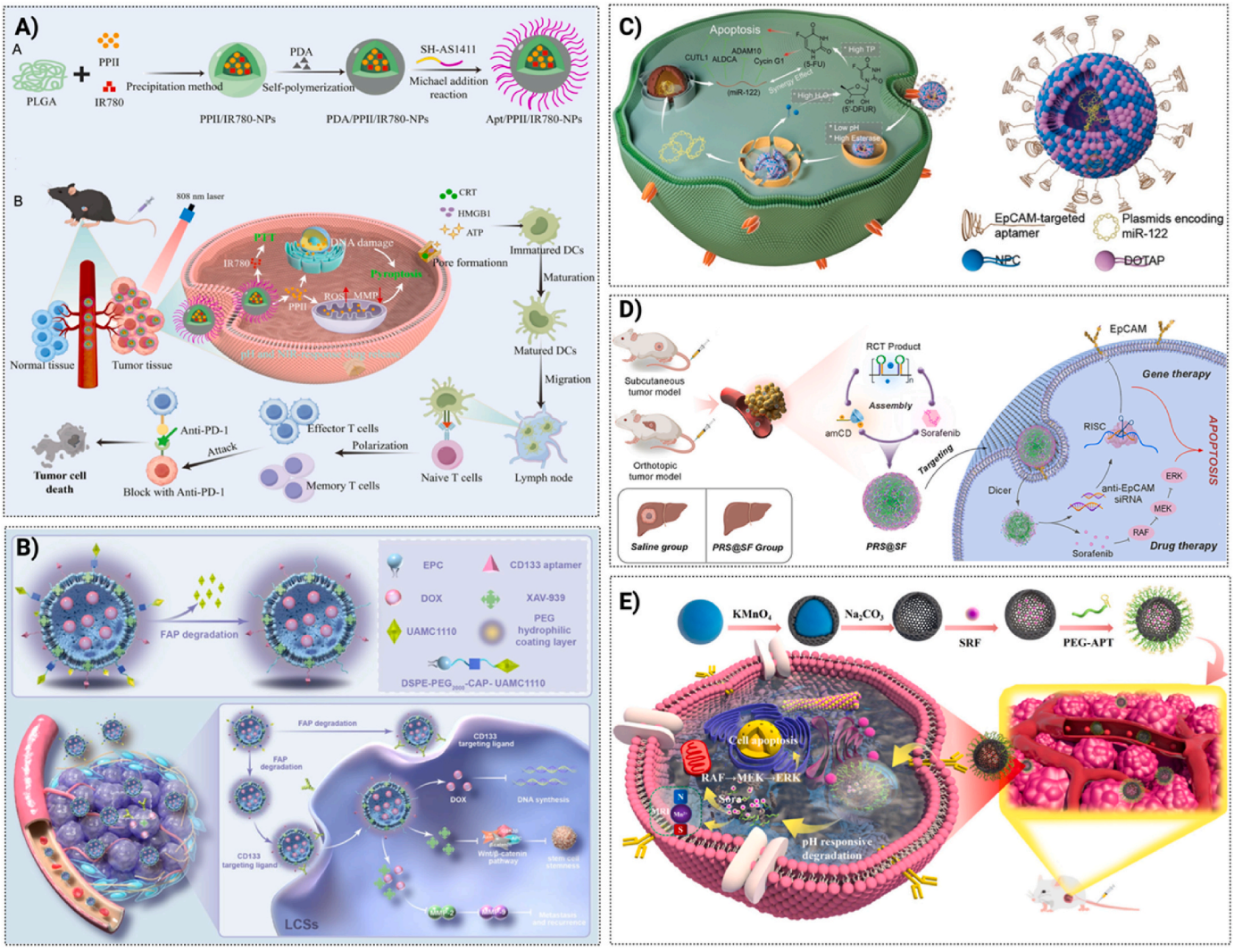

Fig. 5. Aptamer-based targeted therapy strategies in HCC. Schematic illustration of **A)** phyto-chemotherapy approach using AS1411 aptamer for the delivery of polyphyllin II (reprinted from open access Ref. [151]); **B)** targeted therapy using CD133 specific aptamer for the inhibition of metastasis in advanced HCC (reprinted with permission from Ref. [172]); gene and chemotherapy using EPCAM aptamer for the delivery of **C)** doxifluridine and miR-122 (reprinted with permission from Ref. [168]); **D)** sorafenib-loaded porous RNA nanospheres incorporating siRNA (reprinted with permission from Ref. [167]); **E)** theranostic approach using GPC3 aptamer for both diagnosis and treatment with sorafenib (reprinted from open access Ref. [171]).

immunogenicity, enhances nuclease resistance, and improves cellular uptake. By targeting nucleolin, AS1411 demonstrated anti-proliferative effects through multiple pathways. Phase I trials confirmed its safety, but phase II trials for renal cell carcinoma were discontinued due to low efficacy. Despite promising early results in acute myeloid leukemia, further studies were halted [193]. Clinical results for AS1411 in over 100 patients showed no severe side effects with continuous infusion of up to 40 mg/kg/day for 7 days. Although the overall response rate was low, at least 7 patients (3 with renal cell carcinoma and 4 with acute myeloid leukemia) experienced substantial and lasting tumor regression or complete remission [194]. Results from the phase II study showed that the aptamer is rapidly cleared for the bloodstream ($t_{1/2}$ = 1.71 h) and reaches a maximum plasma concentration of 25.4 μg/mL at a time to peak (t_{max}) for 44.1 h. The steady-state plasma concentration was 20.6 ± 7.00 μg/mL, which is comparable to the IC_{50} value observed for renal cancer cell lines *in vitro* [195]. However, research continues to optimize AS1411 structure for potential therapeutic use [196].

Spiegelmers, aptamers composed of non-natural *L*-nucleotides, have entered clinical trials for cancer therapy. Their *L*-configuration enhances nuclease resistance and reduces immunogenicity. NOX-A12 (Olaptesed Pegol) targets stromal cell-derived factor-1, inhibiting C-X-C Motif Chemokine Receptor 4 activation, and has reached phase II trials for metastatic colorectal and pancreatic cancer, multiple myeloma, glioblastoma, and chronic lymphocytic leukemia [43,190]. In a phase II clinical trial combining radiotherapy with dose-escalation of NOX-A12 (200/400/600 mg per week), patients with newly diagnosed glioblastoma received a median treatment duration of 23.2 weeks. Progression-free survival (PES) ranged from 58 to 260 days, with a 6-month PES rate of 40 %. Median overall survival ranged between 144 and 562 days. NOX-A12 plasma concentrations reached a steady state in all patients within approximately one week, consistently exceeding 1.5 μM, considered the minimum level necessary to inhibit CXCL-12 mediated cell migration. The treatment was well tolerated, with no dose-limiting toxicities or treatment related deaths reported [197]. NOX-E36 (Emapticap Pegol) is under investigation for treating diabetes and albuminuria. Its mechanism involves neutralizing the human chemokine CCL2 (C–C Motif Ligand 2), also known as Monocyte Chemoattractant Protein-1 [198]. Research focuses on its oncology potential, with preclinical studies showing efficacy in solid tumors like pancreatic and liver cancer [43]. A Phase I clinical trial has recently begun for AST-201, a novel aptamer-drug conjugate, in patients with GPC3-positive advanced solid tumors (NCT06687941). This

development underscores ongoing efforts to refine aptamer-based therapeutics for oncology.

8. Conclusions and future perspectives

DNA and RNA oligonucleotides serve as versatile molecular tools and building blocks in applications such as genome editing and molecular computing, leveraging their ability to recognize and hybridize with complementary sequences. SELEX is a multidisciplinary process, encompassing molecular biology, nucleic acid chemistry, material science, and bioinformatics to develop affinity ligands for diverse targets. Given its complexity, a universally standardized SELEX protocol applicable to all experimental settings remains impractical [199]. The future of aptamer research depends on refining SELEX methodologies and incorporating chemical modifications to enhance stability, scalability, and biocompatibility. While aptamer nanotechnology holds great promise for HCC diagnostics and therapeutics, overcoming current challenges and expanding target diversity will be key to unlocking their full potential. Advanced SELEX methods like CE-SELEX, Non-SELEX, and Microfluidic-SELEX have improved aptamer selection but cannot precisely control binding affinities. Pro-SELEX addresses this gap by combining particle display, magnetic sorting, high-dimensional selection, and bioinformatics. This approach profiles aptamer binding at varying target concentrations within a single selection round. As proof of concept, Pro-SELEX successfully isolated aptamers for human myeloperoxidase with predefined affinities [63], highlighting its potential for selecting aptamers targeting HCC biomarkers.

The continuous advancement of SELEX configurations and aptamer modifications is set to revolutionize molecular recognition, driving the development of next-generation diagnostic and therapeutic tools. As research progresses, aptamers will play a crucial role in overcoming key challenges in HCC diagnosis and treatment.

CRediT authorship contribution statement

Magdolna Casian: Writing – review & editing, Writing – original draft, Visualization, Methodology, Investigation, Formal analysis, Conceptualization. **Ioana Manea:** Writing – review & editing, Writing – original draft, Methodology, Investigation, Formal analysis. **Oana Hosu-Stancioiu:** Writing – review & editing, Writing – original draft, Validation, Methodology, Conceptualization. **María Jesús Lobo Castañón:** Writing – review & editing, Validation, Supervision, Funding acquisition, Conceptualization. **Noemí de-los-Santos-Álvarez:** Writing – review & editing, Writing – original draft, Validation, Supervision, Methodology, Conceptualization. **Cecilia Cristea:** Writing – review & editing, Validation, Supervision, Project administration, Funding acquisition, Conceptualization.

Data availability

No data was used for the research described in the article.

Declaration of competing interest

The authors declare that they have no known competing financial interests or personal relationships that could have appeared to influence the work reported in this paper.

Acknowledgements

This work was supported by the Romanian Ministry of Education and Research, PN-IV-P1-PCE-2023-1104, no.62PCE/January 03, 2025, the Spanish (project PID2021-123183OB-I00), and Principado de Asturias Government (IDE/2024/000677). MC and IM acknowledge Iuliu Haţieganu UMF for internal grants no. 779/1/January 13, 2025 and no. 776/37/January 13, 2025.

Appendix A. Supplementary data

Supplementary data to this article can be found online at https://doi.org/10.1016/j.trac.2025.118346.

Data availability

Data will be made available on request.

References

[1] GLOBOCAN - World health organization. https://gco.iarc.fr/today/en, 2022. (Accessed 28 February 2025).
[2] F. Safri, R. Nguyen, S. Zerehpooshnesfchi, J. George, L. Qiao, Heterogeneity of hepatocellular carcinoma: from mechanisms to clinical implications, Cancer Gene Ther. 31 (2024) 1105–1112, https://doi.org/10.1038/s41417-024-00764-w.
[3] J.M. Llovet, R.K. Kelley, A. Villanueva, A.G. Singal, E. Pikarsky, S. Roayaie, R. Lencioni, K. Koike, J. Zucman-Rossi, R.S. Finn, Hepatocellular carcinoma, Nat. Rev. Dis. Primers 7 (2021) 6, https://doi.org/10.1038/s41572-020-00240-3.
[4] J. Balogh, D. Victor, E.H. Asham, S.G. Burroughs, M. Boktour, A. Saharia, X. Li, M. Ghobrial, H. Monsour, Hepatocellular carcinoma: a review, J. Hepatocell. Carcinoma 3 (2016) 41–53, https://doi.org/10.2147/JHC.S61146.
[5] K.A. McGlynn, J.L. Petrick, H.B. El-Serag, Epidemiology of hepatocellular carcinoma, Hepatology 73 (2021) 4–13, https://doi.org/10.1002/hep.31288.
[6] T. Akinyemiju, S. Abera, M. Ahmed, N. Alam, M.A. Alemayohu, C. Allen, R. Al-Raddadi, N. Alvis-Guzman, Y. Amoako, A. Artaman, T.A. Ayele, A. Barac, I. Bensenor, A. Berhane, Z. Bhutta, J. Castillo-Rivas, A. Chitheer, J.-Y. Choi, B. Cowie, L. Dandona, R. Dandona, S. Dey, D. Dicker, H. Phuc, D.U. Ekwueme, M. E.S. Zaki, F. Fischer, T. Fürst, J. Hancock, S.I. Hay, P. Hotez, S.H. Jee, A. Kasaeian, Y. Khader, Y.-H. Khang, G.A. Kumar, M. Kutz, H. Larson, A. Lopez, R. Lunevicius, R. Malekzadeh, C. McAlinden, T. Meier, W. Mendoza, A. Mokdad, M. Moradi-Lakeh, G. Nagel, Q. Nguyen, G. Nguyen, F. Ogbo, G. Patton, D. M. Pereira, F. Pourmalek, M. Qorbani, A. Radfar, G. Roshandel, J.A. Salomon, J. Sanabria, B. Sartorius, M. Satpathy, M. Sawhney, S. Sepanlou, K. Shackelford, H. Shore, J. Sun, D.T. Mengistu, R. Topór-Madry, B. Tran, K.N. Ukwaja, V. Vlassov, S.E. Vollset, T. Vos, T. Wakayo, E. Weiderpass, A. Werdecker, N. Yonemoto, M. Younis, C. Yu, Z. Zaidi, L. Zhu, C.J.L. Murray, M. Naghavi, C. Fitzmaurice, The burden of primary liver cancer and underlying etiologies from 1990 to 2015 at the global, regional, and national level, JAMA Oncol. 3 (2017) 1683–1691, https://doi.org/10.1001/jamaoncol.2017.3055.
[7] F. Kanwal, J. Kramer, S.M. Asch, M. Chayanupatkul, Y. Cao, H.B. El-Serag, Risk of hepatocellular cancer in HCV patients treated with direct-acting antiviral agents, Gastroenterology 153 (2017) 996–1005.e1, https://doi.org/10.1053/j.gastro.2017.06.012.
[8] C. Estes, H. Razavi, R. Loomba, Z. Younossi, A.J. Sanyal, Modeling the epidemic of nonalcoholic fatty liver disease demonstrates an exponential increase in burden of disease, Hepatology 67 (2018) 123–133, https://doi.org/10.1002/hep.29466.
[9] S. Xie, L. Ai, C. Cui, T. Fu, X. Cheng, F. Qu, W. Tan, Functional aptamer-embedded nanomaterials for diagnostics and therapeutics, ACS Appl. Mater. Interfaces 13 (2021) 9542–9560, https://doi.org/10.1021/acsami.0c19562.
[10] D. Xiang, C. Zheng, S.-F. Zhou, S. Qiao, P.H.-L. Tran, C. Pu, Y. Li, L. Kong, A. Z. Kouzani, J. Lin, K. Liu, L. Li, S. Shigdar, W. Duan, Superior performance of aptamer in tumor penetration over antibody: implication of aptamer-based theranostics in solid tumors, Theranostics 5 (2015) 1083–1097, https://doi.org/10.7150/thno.11711.
[11] X. Yin, J. Rong, M. Shao, S. Zhang, L. Yin, Z. He, X. Wang, Aptamer-functionalized nanomaterials (AFNs) for therapeutic management of hepatocellular carcinoma, J. Nanobiotechnol. 22 (2024) 243, https://doi.org/10.1186/s12951-024-02486-5.
[12] A. Di Ruscio, V. de Franciscis, Minding the gap: unlocking the therapeutic potential of aptamers and making up for lost time, Mol. Ther. Nucleic Acids 29 (2022) 384–386, https://doi.org/10.1016/j.omtn.2022.07.012.
[13] T. Hennedige, Advances in computed tomography and magnetic resonance imaging of hepatocellular carcinoma, World J. Gastroenterol. 22 (2016) 205–220, https://doi.org/10.3748/wjg.v22.i1.205.
[14] E. Kim, P. Viatour, Hepatocellular carcinoma: old friends and new tricks, Exp. Mol. Med. 52 (2020) 1898–1907, https://doi.org/10.1038/s12276-020-00527-1.
[15] F. Piñero, M. Dirchwolf, M.G. Pessôa, Biomarkers in hepatocellular carcinoma: diagnosis, prognosis and treatment response assessment, Cells 9 (2020) 1370, https://doi.org/10.3390/cells9061370.
[16] O. Jitpraphawan, W. Ruamtawee, M. Treewatchareekorn, S. Sethasine, Diagnostic and prognostic performances of GALAD score in staging and 1-year mortality of hepatocellular carcinoma: a prospective study, World J. Gastroenterol. 30 (2024) 2343–2353, https://doi.org/10.3748/wjg.v30.i17.2343.
[17] Y.-T. Chan, C. Zhang, J. Wu, P. Lu, L. Xu, H. Yuan, Y. Feng, Z.-S. Chen, N. Wang, Biomarkers for diagnosis and therapeutic options in hepatocellular carcinoma, Mol. Cancer 23 (2024) 189, https://doi.org/10.1186/s12943-024-02101-z.
[18] S. Fares, C.J. Wehrle, H. Hong, K. Sun, C. Jiao, M. Zhang, A. Gross, E. Allkushi, M. Uysal, S. Kamath, W.W. Ma, J. Modaresi Esfeh, M.W. Linganna, M. Khalil, A. Pita, J. Kim, R.M. Walsh, C. Miller, K. Hashimoto, A. Schlegel, D.C.H. Kwon, F. Aucejo, Emerging and clinically accepted biomarkers for hepatocellular carcinoma, Cancers 16 (2024) 1453, https://doi.org/10.3390/cancers16081453.

[19] B. Yu, W. Ma, Biomarker discovery in hepatocellular carcinoma (HCC) for personalized treatment and enhanced prognosis, Cytokine Growth Factor Rev. 79 (2024) 29–38, https://doi.org/10.1016/j.cytogfr.2024.08.006.
[20] S.-S. Qiao, Z.-Q.-Q. Cui, L. Gong, H. Han, P.-C. Chen, L.-M. Guo, X. Yu, Y.-H. Wei, S.-A. Ha, J.W. Kim, Z.-T. Jin, S. Li, J.-R. Peng, X.-S. Leng, Simultaneous measurements of serum AFP, GPC-3 and HCCR for diagnosing hepatocellular carcinoma, Hepatogastroenterology 58 (2011) 1718–1724, https://doi.org/10.5754/hge11124.
[21] X. Jia, J. Liu, Y. Gao, Y. Huang, Z. Du, Diagnosis accuracy of serum glypican-3 in patients with hepatocellular carcinoma: a systematic review with meta-analysis, Arch. Med. Res. 45 (2014) 580–588, https://doi.org/10.1016/j.arcmed.2014.11.002.
[22] K.-S. Jeng, I.-S. Sheen, S.-S. Lin, C.-M. Leu, C.-F. Chang, The role of endoglin in hepatocellular carcinoma, Int. J. Mol. Sci. 22 (2021) 3208, https://doi.org/10.3390/ijms22063208.
[23] X. Guo, L. Xiong, L. Yu, R. Li, Z. Wang, B. Ren, J. Dong, B. Li, D. Wang, Increased level of nucleolin confers to aggressive tumor progression and poor prognosis in patients with hepatocellular carcinoma after hepatectomy, Diagn. Pathol. 9 (2014) 175, https://doi.org/10.1186/s13000-014-0175-y.
[24] M. Krizanac, P.B. Mass Sanchez, R. Weiskirchen, A. Asimakopoulos, A scoping review on lipocalin-2 and its role in non-alcoholic steatohepatitis and hepatocellular carcinoma, Int. J. Mol. Sci. 22 (2021) 2865, https://doi.org/10.3390/ijms22062865.
[25] T. Setayesh, S.D. Colquhoun, Y.-J.Y. Wan, Overexpression of galectin-1 and galectin-3 in hepatocellular carcinoma, Liver Res 4 (2020) 173–179, https://doi.org/10.1016/j.livres.2020.11.001.
[26] C.-Y. Hsu, P.-H. Liu, Y.-H. Lee, C.-Y. Hsia, Y.-H. Huang, H.-C. Lin, Y.-Y. Chiou, F.-Y. Lee, T.-I. Huo, Using serum α-fetoprotein for prognostic prediction in patients with hepatocellular carcinoma: what is the most optimal cutoff? PLoS One 10 (2015) e0118825 https://doi.org/10.1371/journal.pone.0118825.
[27] A.S. Lok, R.K. Sterling, J.E. Everhart, E.C. Wright, J.C. Hoefs, A.M. Di Bisceglie, T. R. Morgan, H. Kim, W.M. Lee, H.L. Bonkovsky, J.L. Dienstag, Des-γ-carboxy prothrombin and α-fetoprotein as biomarkers for the early detection of hepatocellular carcinoma, Gastroenterology 138 (2010) 493–502, https://doi.org/10.1053/j.gastro.2009.10.031.
[28] T. Ge, Q. Shen, N. Wang, Y. Zhang, Z. Ge, W. Chu, X. Lv, F. Zhao, W. Zhao, J. Fan, W. Qin, Diagnostic values of alpha-fetoprotein, dickkopf-1, and osteopontin for hepatocellular carcinoma, Med. Oncol. 32 (2015) 59, https://doi.org/10.1007/s12032-014-0367-z.
[29] A. Kasprzak, A. Adamek, Role of endoglin (CD105) in the progression of hepatocellular carcinoma and anti-angiogenic therapy, Int. J. Mol. Sci. 19 (2018) 3887, https://doi.org/10.3390/ijms19123887.
[30] L. Yang, W. Rong, T. Xiao, Y. Zhang, B. Xu, Y. Liu, L. Wang, F. Wu, J. Qi, X. Zhao, H. Wang, N. Han, S. Guo, J. Wu, Y. Gao, S. Cheng, Secretory/releasing proteome-based identification of plasma biomarkers in HBV-associated hepatocellular carcinoma, Sci. China Life Sci. 56 (2013) 638–646, https://doi.org/10.1007/s11427-013-4497-x.
[31] P. Liu, D. Lu, A. Al-ameri, X. Wei, S. Ling, J. Li, H. Zhu, H. Xie, L. Zhu, S. Zheng, X. Xu, Glutamine synthetase promotes tumor invasion in hepatocellular carcinoma through mediating epithelial–mesenchymal transition, Hepatol. Res. 50 (2020) 246–257, https://doi.org/10.1111/hepr.13433.
[32] R. Tenchov, A.K. Sapra, J. Sasso, K. Ralhan, A. Tummala, N. Azoulay, Q.A. Zhou, Biomarkers for early cancer detection: a landscape view of recent advancements, spotlighting pancreatic and liver cancers, ACS Pharmacol. Transl. Sci. 7 (2024) 586–613, https://doi.org/10.1021/acsptsci.3c00346.
[33] M. Liu, Y. Wen, Point-of-care testing for early-stage liver cancer diagnosis and personalized medicine: biomarkers, current technologies and perspectives, Heliyon 10 (2024) e38444, https://doi.org/10.1016/j.heliyon.2024.e38444.
[34] F. Chen, J. Wang, Y. Wu, Q. Gao, S. Zhang, Potential biomarkers for liver cancer diagnosis based on multi-omics strategy, Front. Oncol. 12 (2022) 822449, https://doi.org/10.3389/fonc.2022.822449.
[35] J. He, X. Hu, L. Chen, Y. Jiang, Application of multi-omics in hepatocellular carcinoma: new prospects for classification and precise diagnosis and treatment, Hepatoma. Res. 11 (2025), https://doi.org/10.20517/2394-5079.2024.124.
[36] R.B. Ladju, D. Pascut, M.N. Massi, C. Tiribelli, C.H.C. Sukowati, Correction: aptamer: a potential oligonucleotide nanomedicine in the diagnosis and treatment of hepatocellular carcinoma, Oncotarget 9 (2018) 13101, https://doi.org/10.18632/oncotarget.24572, 13101.
[37] M. Kudo, R.S. Finn, S. Qin, K.-H. Han, K. Ikeda, F. Piscaglia, A. Baron, J.-W. Park, G. Han, J. Jassem, J.F. Blanc, A. Vogel, D. Komov, T.R.J. Evans, C. Lopez, C. Dutcus, M. Guo, K. Saito, S. Kraljevic, T. Tamai, M. Ren, A.-L. Cheng, Lenvatinib versus sorafenib in first-line treatment of patients with unresectable hepatocellular carcinoma: a randomised phase 3 non-inferiority trial, Lancet 391 (2018) 1163–1173, https://doi.org/10.1016/S0140-6736(18)30207-1.
[38] R.S. Finn, S. Qin, M. Ikeda, P.R. Galle, M. Ducreux, T.-Y. Kim, M. Kudo, V. Breder, P. Merle, A.O. Kaseb, D. Li, W. Verret, D.-Z. Xu, S. Hernandez, J. Liu, C. Huang, S. Mulla, Y. Wang, H.Y. Lim, A.X. Zhu, A.-L. Cheng, Atezolizumab plus bevacizumab in unresectable hepatocellular carcinoma, N. Engl. J. Med. 382 (2020) 1894–1905, https://doi.org/10.1056/NEJMoa1915745.
[39] A.-L. Cheng, S. Qin, M. Ikeda, P.R. Galle, M. Ducreux, T.-Y. Kim, H.Y. Lim, M. Kudo, V. Breder, P. Merle, A.O. Kaseb, D. Li, W. Verret, N. Ma, A. Nicholas, Y. Wang, L. Li, A.X. Zhu, R.S. Finn, Updated efficacy and safety data from IMbrave150: atezolizumab plus bevacizumab vs. sorafenib for unresectable hepatocellular carcinoma, J. Hepatol. 76 (2022) 862–873, https://doi.org/10.1016/j.jhep.2021.11.030.
[40] M. Le Grazie, M.R. Biagini, M. Tarocchi, S. Polvani, A. Galli, Chemotherapy for hepatocellular carcinoma: the present and the future, World J. Hepatol. 9 (2017) 907–920, https://doi.org/10.4254/wjh.v9.i21.907.
[41] J.M. Llovet, R. Montal, D. Sia, R.S. Finn, Molecular therapies and precision medicine for hepatocellular carcinoma, Nat. Rev. Clin. Oncol. 15 (2018) 599–616, https://doi.org/10.1038/s41571-018-0073-4.
[42] S. Arshavsky-Graham, C. Heuer, X. Jiang, E. Segal, Aptasensors versus immunosensors—Which will prevail? Eng. Life Sci. 22 (2022) 319–333, https://doi.org/10.1002/elsc.202100148.
[43] F. Mahmoudian, A. Ahmari, S. Shabani, B. Sadeghi, S. Fahimirad, F. Fattahi, Aptamers as an approach to targeted cancer therapy, Cancer Cell Int. 24 (2024) 108, https://doi.org/10.1186/s12935-024-03295-4.
[44] D. Sanjanwala, V. Patravale, Aptamers and nanobodies as alternatives to antibodies for ligand-targeted drug delivery in cancer, Drug Discov. Today 28 (2023) 103550, https://doi.org/10.1016/j.drudis.2023.103550.
[45] A.D. Ellington, J.W. Szostak, In vitro selection of RNA molecules that bind specific ligands, Nature 346 (1990) 818–822, https://doi.org/10.1038/346818a0.
[46] C. Tuerk, L. Gold, Systematic evolution of ligands by exponential enrichment: RNA ligands to bacteriophage T4 DNA polymerase, Science 249 (1990) 505–510, https://doi.org/10.1126/science.2200121.
[47] S. Arshavsky-Graham, K. Urmann, R. Salama, N. Massad-Ivanir, J.-G. Walter, T. Scheper, E. Segal, Aptamers vs. antibodies as capture probes in optical porous silicon biosensors, Analyst 145 (2020) 4991–5003, https://doi.org/10.1039/D0AN00178C.
[48] T. Hermann, D.J. Patel, Adaptive recognition by nucleic acid aptamers, Science 287 (2000) 820–825, https://doi.org/10.1126/science.287.5454.820.
[49] M.C. DeRosa, A. Lin, P. Mallikaratchy, E.M. McConnell, M. McKeague, R. Patel, S. Shigdar, In vitro selection of aptamers and their applications, Nat. Rev. Methods Primers 3 (2023) 54, https://doi.org/10.1038/s43586-023-00238-7.
[50] N.K. Singh, Y. Wang, C. Wen, B. Davis, X. Wang, K. Lee, Y. Wang, High-affinity one-step aptamer selection using a non-fouling porous hydrogel, Nat. Biotechnol. 42 (2024) 1224–1231, https://doi.org/10.1038/s41587-023-01973-8.
[51] K. Yang, O. Alkhamis, J. Canoura, A. Bryant, E.M. Gong, M. Barbu, S. Taylor, D. Nikic, S. Banerjee, Y. Xiao, M.N. Stojanovic, D.W. Landry, Exploring the landscape of aptamers: from cross-reactive to selective to specific, high-affinity receptors for cocaine, JACS Au 4 (2024) 760–770, https://doi.org/10.1021/jacsau.3c00781.
[52] A. Díaz-Fernández, R. Miranda-Castro, N. Díaz, D. Suárez, N. de-los-Santos-Álvarez, M.J. Lobo-Castañón, Aptamers targeting protein-specific glycosylation in tumor biomarkers: general selection, characterization and structural modeling, Chem. Sci. 11 (2020) 9402–9413, https://doi.org/10.1039/D0SC00209G.
[53] A. Díaz-Fernández, R. Miranda-Castro, N. de-los-Santos-Álvarez, M.J. Lobo-Castañón, P. Estrela, Impedimetric aptamer-based glycan PSA score for discrimination of prostate cancer from other prostate diseases, Biosens. Bioelectron. 175 (2021) 112872, https://doi.org/10.1016/j.bios.2020.112872.
[54] A. Stuber, N. Nakatsuka, Aptamer renaissance for neurochemical biosensing, ACS Nano 18 (2024) 13450, https://doi.org/10.1021/acsnano.4c04993.
[55] M.R. Dunn, R.M. Jimenez, J.C. Chaput, Analysis of aptamer discovery and technology, Nat. Rev. Chem 1 (2017) 76, https://doi.org/10.1038/s41570-017-0076.
[56] S. Ni, Z. Zhuo, Y. Pan, Y. Yu, F. Li, J. Liu, L. Wang, X. Wu, D. Li, Y. Wan, L. Zhang, Z. Yang, B.T. Zhang, A. Lu, G. Zhang, Recent progress in aptamer discoveries and modifications for therapeutic applications, ACS Appl. Mater. Interfaces 13 (2021) 9500–9519, https://doi.org/10.1021/acsami.0c05750.
[57] J.G. Bruno, J.L. Kiel, Use of magnetic beads in selection and detection of biotoxin aptamers by electrochemiluminescence and enzymatic methods, Biotechniques 32 (2002) 178–183, https://doi.org/10.2144/02321dd04.
[58] S.D. Mendonsa, M.T. Bowser, In vitro evolution of functional DNA using capillary electrophoresis, J. Am. Chem. Soc. 126 (2004) 20–21, https://doi.org/10.1021/ja037832s.
[59] J. Yang, M.T. Bowser, Capillary electrophoresis-SELEX selection of catalytic DNA aptamers for a small-molecule porphyrin target, Anal. Chem. 85 (2013) 1525–1530, https://doi.org/10.1021/ac302721j.
[60] X. Lou, J. Qian, Y. Xiao, L. Viel, A.E. Gerdon, E.T. Lagally, P. Atzberger, T. M. Tarasow, A.J. Heeger, H.T. Soh, Micromagnetic selection of aptamers in microfluidic channels, Proc. Natl. Acad. Sci. USA 106 (2009) 2989–2994, https://doi.org/10.1073/pnas.0813135106.
[61] J. Wang, Q. Gong, N. Maheshwari, M. Eisenstein, M.L. Arcila, K.S. Kosik, H. T. Soh, Particle display: a quantitative screening method for generating high-affinity aptamers, Angew. Chem. Int. Ed. 53 (2014) 4796–4801, https://doi.org/10.1002/anie.201309334.
[62] A.M. Yoshikawa, L. Wan, L. Zheng, M. Eisenstein, H.T. Soh, A system for multiplexed selection of aptamers with exquisite specificity without counterselection, Proc. Natl. Acad. Sci. USA 119 (2022) e2119945119, https://doi.org/10.1073/pnas.2119945119.
[63] D. Chang, Z. Wang, C.D. Flynn, A. Mahmud, M. Labib, H. Wang, A. Geraili, X. Li, J. Zhang, E.H. Sargent, S.O. Kelley, A high-dimensional microfluidic approach for selection of aptamers with programmable binding affinities, Nat. Chem. 15 (2023) 773–780, https://doi.org/10.1038/s41557-023-01207-z.
[64] A. Bashir, Q. Yang, J. Wang, S. Hoyer, W. Chou, C. McLean, G. Davis, Q. Gong, Z. Armstrong, J. Jang, H. Kang, A. Pawlosky, A. Scott, G.E. Dahl, M. Berndl, M. Dimon, B.S. Ferguson, Machine learning guided aptamer refinement and discovery, Nat. Commun. 12 (2021) 2366, https://doi.org/10.1038/s41467-021-22555-9.

[65] X. Yang, C.H. Chan, S. Yao, H.Y. Chu, M. Lyu, Z. Chen, H. Xiao, Y. Ma, S. Yu, F. Li, J. Liu, L. Wang, Z. Zhang, B.-T. Zhang, L. Zhang, A. Lu, Y. Wang, G. Zhang, Y. Yu, DeepAptamer: advancing high-affinity aptamer discovery with a hybrid deep learning model, Mol. Ther. Nucleic Acids 36 (2025) 102436, https://doi.org/10.1016/j.omtn.2024.102436.
[66] J. Han, L. Gao, J. Wang, J. Wang, Application and development of aptamer in cancer: from clinical diagnosis to cancer therapy, J. Cancer 11 (2020) 6902–6915, https://doi.org/10.7150/jca.49532.
[67] Y. Zhong, J. Zhao, J. Li, X. Liao, F. Chen, Advances of aptamers screened by Cell-SELEX in selection procedure, cancer diagnostics and therapeutics, Anal. Biochem. 598 (2020) 113620, https://doi.org/10.1016/j.ab.2020.113620.
[68] L. Dong, Q. Tan, W. Ye, D. Liu, H. Chen, H. Hu, D. Wen, Y. Liu, Y. Cao, J. Kang, J. Fan, W. Guo, W. Wu, Screening and identifying a novel ssDNA aptamer against alpha-fetoprotein using CE-SELEX, Sci. Rep. 5 (2015) 15552, https://doi.org/10.1038/srep15552.
[69] C.J. Huang, H.I. Lin, S.C. Shiesh, G. Bin Lee, An integrated microfluidic system for rapid screening of alpha-fetoprotein-specific aptamers, Biosens. Bioelectron. 35 (2012) 50–55, https://doi.org/10.1016/j.bios.2012.02.024.
[70] Y.H. Chen, H.I. Lin, C.J. Huang, S.C. Shiesh, G. Bin Lee, An automatic microfluidic system that continuously performs the systematic evolution of ligands by exponential enrichment, Microfluid. Nanofluidics 13 (2012) 929–939, https://doi.org/10.1007/s10404-012-1013-8.
[71] Y.J. Lee, S.W. Lee, Regression of hepatocarcinoma cells using RNA aptamer specific to alpha-fetoprotein, Biochem. Biophys. Res. Commun. 417 (2012) 521–527, https://doi.org/10.1016/j.bbrc.2011.11.153.
[72] J. Du, J. Hong, C. Xu, Y. Cai, B. Xiang, C. Zhou, X. Xu, Screening and identification of ssDNA aptamer for human GP73, BioMed Res. Int. 2015 (2015) 610281, https://doi.org/10.1155/2015/610281.
[73] H. Yan, X. Gao, Y. Zhang, W. Chang, J. Li, X. Li, Q. Du, C. Li, Imaging tiny hepatic tumor xenografts via endoglin-targeted paramagnetic/optical nanoprobe, ACS Appl. Mater. Interfaces 10 (2018) 17047–17057, https://doi.org/10.1021/acsami.8b02648.
[74] M. Zhao, L. Dong, Z. Liu, S. Yang, W. Wu, J. Lin, In vivo fluorescence imaging of hepatocellular carcinoma using a novel GPC3-specific aptamer probe, Quant. Imag. Med. Surg. 8 (2018) 151, https://doi.org/10.21037/qims.2018.01.09.
[75] Y. Zhou, W. Li, Y. Tseng, J. Zhang, J. Liu, Developing slow-off dickkopf-1 aptamers for early-diagnosis of hepatocellular carcinoma, Talanta 194 (2019) 422–429, https://doi.org/10.1016/j.talanta.2018.10.014.
[76] S. Wang, C. Zhang, G. Wang, B. Cheng, Y. Wang, F. Chen, Y. Chen, M. Feng, B. Xiong, Aptamer-mediated transparent-biocompatible nanostructured surfaces for hepotocellular circulating tumor cells enrichment, Theranostics 6 (2016) 1877–1886, https://doi.org/10.7150/thno.15284.
[77] K.A. Lee, J.Y. Ahn, S.H. Lee, S. Singh Sekhon, D.G. Kim, J. Min, Y.H. Kim, Aptamer-based sandwich assay and its clinical outlooks for detecting lipocalin-2 in hepatocellular carcinoma (HCC), Sci. Rep. 5 (2015) 10897, https://doi.org/10.1038/srep10897.
[78] Y.T. Tsai, C.H. Liang, J.H. Yu, K.C. Huang, C.H. Tung, J.E. Wu, Y.Y. Wu, C. H. Chang, T.M. Hong, Y.L. Chen, A DNA aptamer targeting galectin-1 as a novel immunotherapeutic strategy for lung cancer, Mol. Ther. Nucleic Acids 18 (2019) 991–998, https://doi.org/10.1016/j.omtn.2019.10.029.
[79] D. Shangguan, L. Meng, Z.C. Cao, Z. Xiao, X. Fang, Y. Li, D. Cardona, R.P. Witek, C. Liu, W. Tan, Identification of liver cancer-specific aptamers using whole live cells, Anal. Chem. 80 (2008) 721–728, https://doi.org/10.1021/ac701962v.
[80] Y. Rong, H. Chen, X.F. Zhou, C.Q. Yin, B.C. Wang, C.W. Peng, S.P. Liu, F.B. Wang, Identification of an aptamer through whole cell-SELEX for targeting high metastatic liver cancers, Oncotarget 7 (2016) 8282, https://doi.org/10.18632/oncotarget.6988.
[81] L. Zhang, L. Zhou, H. Zhang, Y. Zhang, L. Li, T. Xie, Y. Chen, X. Li, N. Ling, J. Dai, X. Sun, J. Liu, J. Zhao, T. Peng, M. Ye, Development of a DNA aptamer against multidrug-resistant hepatocellular carcinoma for in vivo imaging, ACS Appl. Mater. Interfaces 13 (2021) 54656–54664, https://doi.org/10.1021/acsami.1c12391.
[82] T. Wang, W.X. Chen, G.F. Xu, B. Zhang, S.Q. Wei, J. Hu, K.H. Zhang, A universal strategy designed for selecting bench-to-bedside aptamers to serum and validated in hepatocellular carcinoma diagnosis, Microchem. J. 150 (2019) 104152, https://doi.org/10.1016/j.microc.2019.104152.
[83] A. Brown, J. Brill, R. Amini, C. Nurmi, Y. Li, Development of better aptamers: structured library approaches, selection methods, and chemical modifications, Angew. Chem. Int. Ed. 63 (2024) e202318665, https://doi.org/10.1002/anie.202318665.
[84] M. Kohlberger, G. Gadermaier, SELEX: critical factors and optimization strategies for successful aptamer selection, Biotechnol. Appl. Biochem. 69 (2021) 1771–1792, https://doi.org/10.1002/bab.2244.
[85] I. Manea, M. Casian, O. Hosu-Stancioiu, N. de-los-Santos-Álvarez, M.J. Lobo-Castañón, C. Cristea, A review on magnetic beads-based SELEX technologies: applications from small to large target molecules, Anal. Chim. Acta 1297 (2024) 342325, https://doi.org/10.1016/j.aca.2024.342325.
[86] J.R. Kanwar, K. Roy, R.K. Kanwar, Chimeric aptamers in cancer cell-targeted drug delivery, Crit. Rev. Biochem. Mol. Biol. 46 (2011) 459–477, https://doi.org/10.3109/10409238.2011.614592.
[87] R. Baghban, L. Roshangar, R. Jahanban-Esfahlan, K. Seidi, A. Ebrahimi-Kalan, M. Jaymand, S. Kolahian, T. Javaheri, P. Zare, Tumor microenvironment complexity and therapeutic implications at a glance, cell commun, Signal. 18 (2020) 59, https://doi.org/10.1186/s12964-020-0530-4.
[88] M.J. Mitchell, M.M. Billingsley, R.M. Haley, M.E. Wechsler, N.A. Peppas, R. Langer, Engineering precision nanoparticles for drug delivery, Nat. Rev. Drug Discov. 20 (2021) 101–124, https://doi.org/10.1038/s41573-020-0090-8.
[89] L. Sun, H. Liu, Y. Ye, Y. Lei, R. Islam, S. Tan, R. Tong, Y.-B. Miao, L. Cai, Smart nanoparticles for cancer therapy, Signal Transduct. Targeted Ther. 8 (2023) 418, https://doi.org/10.1038/s41392-023-01642-x.
[90] R. Joy, J. George, F. John, Brief outlook on polymeric nanoparticles, micelles, niosomes, hydrogels and liposomes: preparative methods and action, ChemistrySelect 7 (2022) e202104045, https://doi.org/10.1002/slct.202104045.
[91] H. Cabral, K. Miyata, K. Osada, K. Kataoka, Block copolymer micelles in nanomedicine applications, Chem. Rev. 118 (2018) 6844–6892, https://doi.org/10.1021/acs.chemrev.8b00199.
[92] T.M. Allen, P.R. Cullis, Liposomal drug delivery systems: from concept to clinical applications, Adv. Drug Deliv. Rev. 65 (2013) 36–48, https://doi.org/10.1016/j.addr.2012.09.037.
[93] M. Swierczewska, S. Lee, X. Chen, Inorganic nanoparticles for multimodal molecular imaging, Mol. Imaging 10 (2011) 3–16, https://doi.org/10.2310/7290.2011.00001.
[94] J.J. Giner-Casares, M. Henriksen-Lacey, M. Coronado-Puchau, L.M. Liz-Marzán, Inorganic nanoparticles for biomedicine: where materials scientists meet medical research, Mater. Today 19 (2016) 19–28, https://doi.org/10.1016/j.mattod.2015.07.004.
[95] S. Senapati, A.K. Mahanta, S. Kumar, P. Maiti, Controlled drug delivery vehicles for cancer treatment and their performance, Signal Transduct. Targeted Ther. 3 (2018) 7, https://doi.org/10.1038/s41392-017-0004-3.
[96] R. Bilan, I. Nabiev, A. Sukhanova, Quantum dot-based nanotools for bioimaging, diagnostics, and drug delivery, Chembiochem 17 (2016) 2103–2114, https://doi.org/10.1002/cbic.201600357.
[97] S. Senapati, R. Thakur, S.P. Verma, S. Duggal, D.P. Mishra, P. Das, T. Shripathi, M. Kumar, D. Rana, P. Maiti, Layered double hydroxides as effective carrier for anticancer drugs and tailoring of release rate through interlayer anions, J. Contr. Release 224 (2016) 186–198, https://doi.org/10.1016/j.jconrel.2016.01.016.
[98] D. Lombardo, M.A. Kiselev, M.T. Caccamo, Smart nanoparticles for drug delivery application: development of versatile nanocarrier platforms in biotechnology and nanomedicine, J. Nanomater. 2019 (2019) 1–26, https://doi.org/10.1155/2019/3702518.
[99] Y. Li, C. Vulpe, T. Lammers, R.M. Pallares, Assessing inorganic nanoparticle toxicity through omics approaches, Nanoscale 16 (2024) 15928–15945, https://doi.org/10.1039/D4NR02328E.
[100] L.S. Arias, J.P. Pessan, A.P.M. Vieira, T.M.T. de Lima, A.C.B. Delbem, D. R. Monteiro, Iron oxide nanoparticles for biomedical applications: a perspective on synthesis, drugs, antimicrobial activity, and toxicity, Antibiotics 7 (2018) 46, https://doi.org/10.3390/antibiotics7020046.
[101] J. Nowak-Jary, B. Machnicka, Pharmacokinetics of magnetic iron oxide nanoparticles for medical applications, J. Nanobiotechnol. 20 (2022) 305, https://doi.org/10.1186/s12951-022-01510-w.
[102] D.-W. Han, S.C. Hong, J.H. Lee, J. Lee, H.Y. Kim, J.Y. Park, Cho, J. Lee, D.-W. Han, Subtle cytotoxicity and genotoxicity differences in superparamagnetic iron oxide nanoparticles coated with various functional groups, Int. J. Nanomed. 3219 (2011), https://doi.org/10.2147/IJN.S26355.
[103] R. Mohammadpour, M.A. Dobrovolskaia, D.L. Cheney, K.F. Greish, H. Ghandehari, Subchronic and chronic toxicity evaluation of inorganic nanoparticles for delivery applications, Adv. Drug Deliv. Rev. 144 (2019) 112–132, https://doi.org/10.1016/j.addr.2019.07.006.
[104] M.R. Miller, J.B. Raftis, J.P. Langrish, S.G. McLean, P. Samutrtai, S.P. Connell, S. Wilson, A.T. Vesey, P.H.B. Fokkens, A.J.F. Boere, P. Krystek, C.J. Campbell, P. W.F. Hadoke, K. Donaldson, F.R. Cassee, D.E. Newby, R. Duffin, N.L. Mills, Inhaled nanoparticles accumulate at sites of vascular disease, ACS Nano 11 (2017) 4542–4552, https://doi.org/10.1021/acsnano.6b08551.
[105] E. Musielak, V. Krajka-Kuźniak, Lipidic and inorganic nanoparticles for targeted glioblastoma multiforme therapy: advances and strategies, Micro 5 (2025) 2, https://doi.org/10.3390/micro5010002.
[106] F. Odeh, H. Nsairat, W. Alshaer, M.A. Ismail, E. Esawi, B. Qaqish, A. Al Bawab, S. I. Ismail, Aptamers chemistry: chemical modifications and conjugation strategies, Molecules 25 (2019) 3, https://doi.org/10.3390/molecules25010003.
[107] M. Heiat, M. Negahdary, Sensitive diagnosis of alpha-fetoprotein by a label free nanoaptasensor designed by modified Au electrode with spindle-shaped gold nanostructure, Microchem. J. 148 (2019) 456–466, https://doi.org/10.1016/j.microc.2019.05.004.
[108] G. Li, S. Li, Z. Wang, Y. Xue, C. Dong, J. Zeng, Y. Huang, J. Liang, Z. Zhou, Label-free electrochemical aptasensor for detection of alpha-fetoprotein based on AFP-aptamer and thionin/reduced graphene oxide/gold nanoparticles, Anal. Biochem. 547 (2018) 37–44, https://doi.org/10.1016/j.ab.2018.02.012.
[109] G. Li, W. Li, S. Li, X. Shi, J. Liang, J. Lai, Z. Zhou, A novel aptasensor based on light-addressable potentiometric sensor for the determination of Alpha-fetoprotein, Biochem. Eng. J. 164 (2020) 107780, https://doi.org/10.1016/j.bej.2020.107780.
[110] H. Zhao, S. Bian, Y. Yang, X. Wu, Chiroplasmonic assemblies of gold nanoparticles as a novel method for sensitive detection of alpha-fetoprotein, Microchim. Acta 184 (2017) 1855–1862, https://doi.org/10.1007/s00604-017-2207-2.
[111] L. Zhou, F. Ji, T. Zhang, F. Wang, Y. Li, Z. Yu, X. Jin, B. Ruan, An fluorescent aptasensor for sensitive detection of tumor marker based on the FRET of a sandwich structured QDs-AFP-AuNPs, Talanta 197 (2019) 444–450, https://doi.org/10.1016/j.talanta.2019.01.012.

[112] M. Ma, M. Zhang, J. Wang, Y. Zhou, X. Zhang, G. Liu, Rapid detection of alpha-fetoprotein (AFP) with lateral flow aptasensor, Molecules 30 (2025) 484, https://doi.org/10.3390/molecules30030484.
[113] W. Li, M. Chen, J. Liang, C. Lu, M. Zhang, F. Hu, Z. Zhou, G. Li, Electrochemical aptasensor for analyzing alpha-fetoprotein using RGO–CS–Fc nanocomposites integrated with gold–platinum nanoparticles, Anal. Methods 12 (2020) 4956–4966, https://doi.org/10.1039/D0AY01465F.
[114] J. Upan, N. Youngvises, A. Tuantranont, C. Karuwan, P. Banet, P.H. Aubert, J. Jakmunee, A simple label-free electrochemical sensor for sensitive detection of alpha-fetoprotein based on specific aptamer immobilized platinum nanoparticles/carboxylated-graphene oxide, Sci. Rep. 11 (2021) 13969, https://doi.org/10.1038/s41598-021-93399-y.
[115] G. Li, J. Zeng, H. Liu, P. Ding, J. Liang, X. Nie, Z. Zhou, A fluorometric aptamer nanoprobe for alpha-fetoprotein by exploiting the FRET between 5-carboxy-fluorescein and palladium nanoparticles, Microchim. Acta 186 (2019) 314, https://doi.org/10.1007/s00604-019-3403-z.
[116] Z. Rahmati, M. Roushani, H. Hosseini, Hierarchical nickel hydroxide nanosheets grown on hollow nitrogen doped carbon nanoboxes as a high-performance surface substrate for alpha-fetoprotein cancer biomarkers electrochemical aptasensing, Talanta 237 (2022) 122924, https://doi.org/10.1016/j.talanta.2021.122924.
[117] Y.-F. Hu, Y.-X. Chen, S.-Y. Chen, Green synthesis of near-infrared carbon dots as a novel aptamer-based fluorescence probe for the detection and imaging of alpha-fetoprotein, Microchim. Acta 192 (2025) 179, https://doi.org/10.1007/s00604-025-07046-8.
[118] H. Zhao, H. Qi, T. Yi, T. Jing, J. Li, S. Shen, Q. Zeng, Y. Gao, Quantum yield of carbon dots adjusts the performance of TiO_2-In_2S_3-based photoelectrochemical biosensor for alpha-fetoprotein detection, Microchem. J. (2025) 113115, https://doi.org/10.1016/j.microc.2025.113115.
[119] X. Wu, P. Fu, W. Ma, L. Xu, H. Kuang, C. Xu, SERS-active silver nanoparticle trimers for sub-attomolar detection of alpha fetoprotein, RSC Adv. 5 (2015) 73395–73398, https://doi.org/10.1039/C5RA12629K.
[120] X. Kang, Z. Peng, Q. Li, Z. Fan, J. Zhang, Y. Song, J. Zhang, Q. Han, Highly stable SERS-based mirrored aptasensor for selective detection of alpha-fetoprotein, Microchim. Acta 192 (2025) 118, https://doi.org/10.1007/s00604-025-06985-6.
[121] A. Qu, X. Wu, L. Xu, L. Liu, W. Ma, H. Kuang, C. Xu, SERS- and luminescence-active Au–Au–UCNP trimers for attomolar detection of two cancer biomarkers, Nanoscale 9 (2017) 3865–3872, https://doi.org/10.1039/C6NR09114H.
[122] X. Sun, F. Fang, J. Na, R. Yan, Y. Huang, Z. Zhou, Y. Zhao, G. Li, Fluorescent "turn-on" aptamer sensor for sensitive and reliable detection of golgi glycoprotein 73 based on nitrogen-doped graphene quantum dots and molybdenum disulfide nanosheets, J. Pharm. Biomed. Anal. 225 (2023) 115215, https://doi.org/10.1016/j.jpba.2022.115215.
[123] J. Liang, R. Yan, C. Chen, X. Yao, F. Guo, R. Wu, Z. Zhou, J. Chen, G. Li, A novel fluorescent strategy for golgi protein 73 determination based on aptamer/nitrogen-doped graphene quantum dots/molybdenum disulfide @ reduced graphene oxide nanosheets, Spectrochim. Acta Mol. Biomol. Spectrosc. 294 (2023) 122538, https://doi.org/10.1016/j.saa.2023.122538.
[124] J. Liang, B. Wan, X. Tan, J. Li, Y. Zhan, Y. Huang, Z. Zhou, G. Li, An electrochemical biosensor based on MoS_2-PANi@Fc for the detection of golgi protein 73, Microchem. J. 205 (2024) 111182, https://doi.org/10.1016/j.microc.2024.111182.
[125] G. Li, R. Yan, W. Chen, R. Wu, J. Liang, J. Chen, Z. Zhou, Fluorescence/electrochemical dual-mode strategy for golgi protein 73 detection based on molybdenum disulfide/ferrocene/palladium nanoparticles and nitrogen-doped graphene quantum dots, Microchim. Acta 191 (2024) 190, https://doi.org/10.1007/s00604-024-06262-y.
[126] X. Li, S. Li, Q. Lv, C. Wang, J. Liang, Z. Zhou, G. Li, Colorimetric biosensor for visual determination of golgi protein 73 based on reduced graphene oxide-carboxymethyl chitosan-hemin/platinum@palladium nanozyme with peroxidase-like activity, Microchim. Acta 189 (2022) 193, https://doi.org/10.1007/s00604-022-05480-6.
[127] G. Li, M. Chen, B. Wang, C. Wang, G. Wu, J. Liang, Z. Zhou, Dual-signal sandwich-type aptasensor based on H-rGO-Mn_3O_4 nanozymes for ultrasensitive golgi protein 73 determination, Anal. Chim. Acta 1221 (2022) 340102, https://doi.org/10.1016/j.aca.2022.340102.
[128] G. Li, B. Wang, S. Li, X. Li, R. Yan, X. Tan, J. Liang, Z. Zhou, Competitive electrochemical aptasensor for high sensitivity detection of liver cancer marker GP73 based on rGO-Fc-PANi nanocomposites, Bioelectrochemistry 160 (2024) 108767, https://doi.org/10.1016/j.bioelechem.2024.108767.
[129] X. Tan, H. Lin, J. Zhou, Z. Su, B. Wan, X. Li, Z. Zhou, Y. Liu, G. Li, Electroactive Hemin-Cu-MOF nanocomposites driven ratiometric electrochemical aptasensor for sensitive golgi protein 73 detection, Sensor. Actuator. B Chem. 423 (2025) 136839, https://doi.org/10.1016/j.snb.2024.136839.
[130] J. Li, B. Wang, S. Gu, Y. Yang, Z. Wang, Y. Xiang, Amperometric low potential aptasensor for the fucosylated golgi protein 73, a marker for hepatocellular carcinoma, Microchim. Acta 184 (2017) 3131–3136, https://doi.org/10.1007/s00604-017-2334-9.
[131] Z. Zhou, L. Zhao, W. Li, M. Chen, H. Feng, X. Shi, J. Liang, G. Li, Glypican-3 electrochemical aptamer nanobiosensor based on hemin/graphene nanohybrids peroxidase-like catalytic silver deposition, Microchim. Acta 187 (2020) 305, https://doi.org/10.1007/s00604-020-04284-w.
[132] G. Li, H. Feng, X. Shi, M. Chen, J. Liang, Z. Zhou, Highly sensitive electrochemical aptasensor for Glypican-3 based on reduced graphene oxide-hemin nanocomposites modified on screen-printed electrode surface, Bioelectrochemistry 138 (2021) 107696, https://doi.org/10.1016/j.bioelechem.2020.107696.
[133] G. Li, B. Wang, L. Zhao, X. Shi, G. Wu, W. Chen, L. Sun, J. Liang, Z. Zhou, Label-free detection of glypican-3 using reduced graphene oxide/polyetherimide/gold nanoparticles enhanced aptamer specific sensing interface on light-addressable potentiometric sensor, Electrochim. Acta 426 (2022) 140808, https://doi.org/10.1016/j.electacta.2022.140808.
[134] G. Li, W. Chen, D. Mi, B. Wang, H.M. Li, G. Wu, P. Ding, J. Liang, Z. Zhou, A highly sensitive strategy for glypican-3 detection based on aptamer/gold carbon dots/magnetic graphene oxide nanosheets as fluorescent biosensor, Anal. Bioanal. Chem. 414 (2022) 6441–6453, https://doi.org/10.1007/s00216-022-04201-5.
[135] X. Shi, M. Chen, H. Feng, Z. Zhou, R. Wu, W. Li, J. Liang, J. Chen, G. Li, Glypican-3 electrochemical aptasensor based on reduced graphene oxide-chitosan-ferrocene deposition of platinum–palladium bimetallic nanoparticles, J. Appl. Electrochem. 51 (2021) 781–794, https://doi.org/10.1007/s10800-021-01534-4.
[136] G. Li, F. Guo, J. Liang, B. Wan, J. Liang, Z. Zhou, Sandwich-type supersensitive electrochemical aptasensor of glypican-3 based on PrGO-Hemin-PdNP and AuNP@PoPD, Microchim. Acta 191 (2024) 340, https://doi.org/10.1007/s00604-024-06419-9.
[137] S. Li, X. Li, L. Cao, C. Wang, J. Liang, Z. Zhou, G. Li, An ultrasensitive glypican 3 electrochemical aptasensor based on reduced graphene oxide-carboxymethylchitosan-hemin/palladium nanoparticles, J. Electrochem. Soc. 169 (2022) 087517, https://doi.org/10.1149/1945-7111/ac8955.
[138] G. Li, H. Feng, X. Li, S. Li, J. Liang, Z. Zhou, A dual-signal output electrochemical aptasensor for glypican-3 ultrasensitive detection based on reduced graphene oxide-cuprous oxide nanozyme catalytic amplification strategy, Bioelectrochemistry 158 (2024) 108709, https://doi.org/10.1016/j.bioelechem.2024.108709.
[139] Y. Jiang, D. Sun, Z. Liang, L. Chen, Y. Zhang, Z. Chen, Label-free and competitive aptamer cytosensor based on layer-by-layer assembly of DNA-platinum nanoparticles for ultrasensitive determination of tumor cells, Sensor. Actuator. B Chem. 262 (2018) 35–43, https://doi.org/10.1016/j.snb.2018.01.194.
[140] D. Wu, Y. Yu, D. Jin, M.M. Xiao, Z.Y. Zhang, G.J. Zhang, Dual-aptamer modified graphene field-effect transistor nanosensor for label-free and specific detection of hepatocellular carcinoma-derived microvesicles, Anal. Chem. 92 (2020) 4006–4015, https://doi.org/10.1021/acs.analchem.9b05531.
[141] G. Liao, X. Liu, X. Yang, Q. Wang, X. Geng, L. Zou, Y. Liu, S. Li, Y. Zheng, K. Wang, Surface plasmon resonance assay for exosomes based on aptamer recognition and polydopamine-functionalized gold nanoparticles for signal amplification, Microchim. Acta 187 (2020) 251, https://doi.org/10.1007/s00604-020-4183-1.
[142] Q. Chen, H. Gao, J. Yao, B. Jiang, R. Yuan, Y. Xiang, Target/aptamer binding-induced inhibition of enzyme activity for amplified electrochemical detection of sonic hedgehog protein, Sensor. Actuator. B Chem. 385 (2023) 133702, https://doi.org/10.1016/j.snb.2023.133702.
[143] C.S.M. Ferreira, C.S. Matthews, S. Missailidis, DNA aptamers that bind to MUC1 tumour marker: design and characterization of MUC1-binding single-stranded DNA aptamers, Tumor Biol. 27 (2006) 289–301, https://doi.org/10.1159/000096085.
[144] X. Wang, W. Li, Z. Li, H. Li, D. Xu, A highly sensitive fluorescence turn-on platform with silver nanoparticles aptasening for human platelet-derived growth factor-BB, Talanta 144 (2015) 1273–1278, https://doi.org/10.1016/j.talanta.2015.07.019.
[145] B. Yu, W. Ma, Biomarker discovery in hepatocellular carcinoma (HCC) for personalized treatment and enhanced prognosis, Cytokine Growth Factor Rev. 79 (2024) 29–38, https://doi.org/10.1016/j.cytogfr.2024.08.006.
[146] S. Zheng, S.W. Chan, F. Liu, J. Liu, P.K.H. Chow, H.C. Toh, S. Zheng, S.W. Chan, F. Liu, J. Liu, P. Kah, H. Chow, H.C. Toh, W. Hong, Hepatocellular carcinoma: current drug therapeutic status, advances and challenges, Cancers 16 (2024) 1582, https://doi.org/10.3390/cancers16081582.
[147] H. Samant, H.S. Amiri, G.B. Zibari, Addressing the worldwide hepatocellular carcinoma: epidemiology, prevention and management, J. Gastrointest. Oncol. 12 (2021) S361–S373, https://doi.org/10.21037/jgo.2020.02.08.
[148] G. Ravichandran, A.K. Rengan, Aptamer-mediated nanotheranostics for cancer treatment: a review, ACS Appl. Nano Mater. 3 (2020) 9542–9559, https://doi.org/10.1021/acsanm.0c01785.
[149] Y. Morita, M. Leslie, H. Kameyama, D.E. Volk, T. Tanaka, Aptamer therapeutics in cancer: current and future, Cancers 10 (2018) 80, https://doi.org/10.3390/cancers10030080.
[150] H. Huang, A. Chang, H. Peng, J. Liu, A. Yao, Y. Ruan, P. Zhang, T. Wang, C. Qu, X. Yin, J. Ni, X. Dong, Preparation and anti-tumor effect in hepatocellular carcinoma treatment of AS1411 aptamer-targeted polyphyllin II-loaded PLGA nanoparticles, J. Sci. Adv. Mater. Devices 9 (2024) 100755, https://doi.org/10.1016/j.jsamd.2024.100755.
[151] H. Huang, J. Fu, H. Peng, Y. He, A. Chang, H. Zhang, Y. Hao, X. Xu, S. Li, J. Zhao, J. Ni, X. Dong, Co-delivery of polyphyllin II and IR780 PLGA nanoparticles induced pyroptosis combined with photothermal to enhance hepatocellular carcinoma immunotherapy, J. Nanobiotechnol. 22 (2024) 647, https://doi.org/10.1186/s12951-024-02887-6.
[152] A.A. Abd-Rabou, H.H. Ahmed, M.S. Kishta, K.M.A. Zoheir, Selective viramidine-loaded aptamer-nanoparticles trigger cell cycle arrest in nucleolin-expressed hepatoma cells through modulation of CDC25A/p53/PI3k pathway, J. Cluster Sci. 34 (2023) 335–348, https://doi.org/10.1007/s10876-022-02224-7.
[153] M. Dhara, A. Al Hoque, R. Sen, D. Dutta, B. Mukherjee, B. Paul, S. Laha, Phosphorothioated amino-AS1411 aptamer functionalized stealth nanoliposome accelerates bio-therapeutic threshold of apigenin in neoplastic rat liver: a mechanistic approach, J. Nanobiotechnol. 21 (2023) 28, https://doi.org/10.1186/s12951-022-01764-4.

[154] X. Liang, Y. Wang, H. Shi, M. Dong, H. Han, Q. Li, Nucleolin-targeting AS1411 aptamer-modified micelle for the co-delivery of doxorubicin and miR-519c to improve the therapeutic efficacy in hepatocellular carcinoma treatment, Int. J. Nanomed. 16 (2021) 2569–2584, https://doi.org/10.2147/IJN.S304526.
[155] T. Le Trinh, G. Zhu, X. Xiao, W. Puszyk, K. Sefah, Q. Wu, W. Tan, C. Liu, A synthetic aptamer-drug adduct for targeted liver cancer therapy, PLoS One 10 (2015) e0136673, https://doi.org/10.1371/journal.pone.0136673.
[156] X. Zhang, Q. Gao, Q. Zhuang, L. Zhang, S. Wang, L. Du, W. Yuan, C. Wang, Q. Tian, H. Yu, Y. Zhao, Y. Liu, A dual-functional nanovehicle with fluorescent tracking and its targeted killing effects on hepatocellular carcinoma cells, RSC Adv. 11 (2021) 10986–10995, https://doi.org/10.1039/D0RA10486H.
[157] X. Zhao, J. Yang, jing Zhang, X. Wang, L. Chen, C. Zhang, Z. Shen, Inhibitory effect of aptamer-carbon dot nanomaterial-siRNA complex on the metastasis of hepatocellular carcinoma cells by interfering with FMRP, Eur. J. Pharm. Biopharm. 174 (2022) 47–55, https://doi.org/10.1016/j.ejpb.2022.03.013.
[158] Z. Ding, D. Wang, W. Shi, X. Yang, S. Duan, F. Mo, X. Hou, A. Liu, X. Lu, In vivo targeting of liver cancer with tissue- and nuclei-specific mesoporous silica nanoparticle-based nanocarriers in mice, Int. J. Nanomed. 15 (2020) 8383–8400, https://doi.org/10.2147/IJN.S272495.
[159] L. Chen, W. Hong, S. Duan, Y. Li, J. Wang, J. Zhu, Graphene quantum dots mediated magnetic chitosan drug delivery nanosystems for targeting synergistic photothermal-chemotherapy of hepatocellular carcinoma, Cancer Biol. Ther. 23 (2022) 281–293, https://doi.org/10.1080/15384047.2022.2054249.
[160] D. Zhang, A. Zheng, J. Li, M. Wu, L. Wu, Z. Wei, N. Liao, X. Zhang, Z. Cai, H. Yang, G. Liu, X. Liu, J. Liu, Smart Cu(II)-aptamer complexes based gold nanoplatform for tumor micro-environment triggered programmable intracellular prodrug release, photodynamic treatment and aggregation induced photothermal therapy of hepatocellular carcinoma, Theranostics 7 (2017) 164–179, https://doi.org/10.7150/thno.17099.
[161] S. Lan, Z. Lin, D. Zhang, Y. Zeng, X. Liu, Photocatalysis enhancement for programmable killing of hepatocellular carcinoma through self-compensation mechanisms based on black phosphorus quantum-dot-hybridized nanocatalysts, ACS Appl. Mater. Interfaces 11 (2019) 9804–9813, https://doi.org/10.1021/acsami.8b21820.
[162] S. Chakraborty, Z.Y. Dlie, S. Chakraborty, S. Roy, B. Mukherjee, S.E. Besra, S. Dewanjee, A. Mukherjee, P.K. Ojha, V. Kumar, R. Sen, Aptamer-functionalized drug nanocarrier improves hepatocellular carcinoma toward normal by targeting neoplastic hepatocytes, Mol. Ther. Nucleic Acids 20 (2020) 34–49, https://doi.org/10.1016/j.omtn.2020.01.034.
[163] C. Pilapong, S. Sitthichai, S. Thongtem, T. Thongtem, Smart magnetic nanoparticle-aptamer probe for targeted imaging and treatment of hepatocellular carcinoma, Int. J. Pharm. 473 (2014) 469–474, https://doi.org/10.1016/j.ijpharm.2014.07.036.
[164] J.Q. Le, X.H. Song, L.W. Tong, Y.Q. Lin, K.K. Feng, Y.F. Tu, Y.S. Hu, J.W. Shao, Dual-drug controllable co-assembly nanosystem for targeted and synergistic treatment of hepatocellular carcinoma, J. Colloid Interface Sci. 656 (2024) 177–188, https://doi.org/10.1016/j.jcis.2023.11.109.
[165] M. Babaei, K. Abnous, S.M. Taghdisi, S.A. Farzad, M.T. Peivandi, M. Ramezani, M. Alibolandi, Synthesis of theranostic epithelial cell adhesion molecule targeted mesoporous silica nanoparticle with gold gatekeeper for hepatocellular carcinoma, Nanomedicine 12 (2017) 1261–1279, https://doi.org/10.2217/nnm-2017-0028.
[166] S. Xiao, Z. Liu, R. Deng, C. Li, S. Fu, G. Chen, X. Zhang, F. Ke, S. Ke, X. Yu, S. Wang, Z. Zhong, Aptamer-mediated gene therapy enhanced antitumor activity against human hepatocellular carcinoma in vitro and in vivo, J. Contr. Release 258 (2017) 130–145, https://doi.org/10.1016/j.jconrel.2017.05.017.
[167] X. Chen, T. Chen, L. Zhang, Z. Wang, Q. Zhou, T. Huang, C. Ge, H. Xu, M. Zhu, F. Zhao, M. Yao, H. Tian, H. Li, X. Zhu, J. Li, Cyclodextrin-mediated formation of porous RNA nanospheres and their application in synergistic targeted therapeutics of hepatocellular carcinoma, Biomaterials 261 (2020) 120304, https://doi.org/10.1016/j.biomaterials.2020.120304.
[168] F. Xue, X. Lin, Z. Cai, X. Liu, Y. Ma, M. Wu, Doxifluridine-based pharmacosomes delivering miR-122 as tumor microenvironments-activated nanoplatforms for synergistic treatment of hepatocellular carcinoma, Colloids Surf. B Biointerfaces 197 (2021) 111367, https://doi.org/10.1016/j.colsurfb.2020.111367.
[169] B.C. Zhang, B.Y. Luo, J.J. Zou, P.Y. Wu, J.L. Jiang, J.Q. Le, R.R. Zhao, L. Chen, J. W. Shao, Co-delivery of sorafenib and CRISPR/Cas9 based on targeted core-shell hollow mesoporous organosilica nanoparticles for synergistic HCC therapy, ACS Appl. Mater. Interfaces 12 (2020) 57362–57372, https://doi.org/10.1021/acsami.0c17660.
[170] M. Zhao, Z. Liu, L. Dong, H. Zhou, S. Yang, W. Wu, J. Lin, A GPC3-specific aptamer-mediated magnetic resonance probe for hepatocellular carcinoma, Int. J. Nanomed. 13 (2018) 4433–4443, https://doi.org/10.2147/IJN.S168268.
[171] Z. Wang, C. Wu, J. Liu, S. Hu, J. Yu, Q. Yin, H. Tian, Z. Ding, G. Qi, L. Wang, L. Hao, Aptamer-mediated hollow MnO_2 for targeting the delivery of sorafenib, Drug Deliv. 30 (2023) 28–39, https://doi.org/10.1080/10717544.2022.2149897.
[172] L. Kong, Y. Yu, R. Yang, R. bo Guo, L. Zhang, J. hua Wang, Y. Liu, J. Zang, C. Yang, H. yue Yang, R. jun Ju, X. tao Li, Development and efficacy evaluation of nanoliposomes targeting CAFs-LCSCs communication for hepatocellular carcinoma treatment, Chem. Eng. J. 496 (2024) 154173, https://doi.org/10.1016/j.cej.2024.154173.
[173] L. Jianghong, M. Tingting, Z. Yingping, Y. Tong, Z. Lanxia, L. Jingwen, Z. Wentao, C. Pengbo, Y. Hong, H. Fuqiang, Aptamer and peptide-modified lipid-based drug delivery systems in application of combined sequential therapy of hepatocellular carcinoma, ACS Biomater. Sci. Eng. 7 (2021) 2558–2568, https://doi.org/10.1021/acsbiomaterials.1c00357.
[174] J. Jiang, H. Chen, C. Yu, Y. Zhang, M. Chen, S. Tian, C. Sun, The promotion of salinomycin delivery to hepatocellular carcinoma cells through EGFR and CD133 aptamers conjugation by PLGA nanoparticles, Nanomedicine 10 (2015) 1863–1879, https://doi.org/10.2217/nnm.15.43.
[175] N. Qiang, L. Wei, Y. Tao, W. Jin, Y. Bin, Z. Dinghua, Construction of durvalumab/carbon nanotube/PEI/aptamer-siRNA chimera for the immunotherapy of hepatocellular carcinoma, Biomed. Mater. 17 (2022), https://doi.org/10.1088/1748-605X/AC5414.
[176] P.J. Bates, D.A. Laber, D.M. Miller, S.D. Thomas, J.O. Trent, Discovery and development of the G-rich oligonucleotide AS1411 as a novel treatment for cancer, Exp. Mol. Pathol. 86 (2009) 151–164, https://doi.org/10.1016/j.yexmp.2009.01.004.
[177] Y. Cho, Y. Bin Lee, J.H. Lee, D.H. Lee, E.J. Cho, S.J. Yu, Y.J. Kim, J.I. Kim, J.H. Im, J.H. Lee, E.J. Oh, J.H. Yoon, Modified AS1411 aptamer suppresses hepatocellular carcinoma by up-regulating galectin-14, PLoS One 11 (2016) e0160822, https://doi.org/10.1371/journal.pone.0160822.
[178] C. Roxo, W. Kotkowiak, A. Pasternak, G-quadruplex-forming aptamers—characteristics, applications, and perspectives, Molecules 24 (2019) 3781, https://doi.org/10.3390/molecules24203781.
[179] S. Kim, K.Y. Lee, H. Kang, S.H. Ryu, D.S. Lee, J.H. Lee, Bioimaging of nucleolin aptamer-containing 5-(N-benzylcarboxyamide)-2′-deoxyuridine more capable of specific binding to targets in cancer cells, BioMed Res. Int. 2010 (2010) 168306, https://doi.org/10.1155/2010/168306.
[180] A. Rezgui, R.A. Tachour, H. Layaida, R. Derguine, F.Z. Hab, A. Benmanseur, B. Matougui, R. Agred, W. Sobhi, Doxorubicin inhibits SIRT2 and NF-kB p65 phosphorylation in breast cell-line cancer, Biochem. Biophys. Res. Commun. 743 (2025) 151162, https://doi.org/10.1016/j.bbrc.2024.151162.
[181] G.M.F. Calixto, S.R. de Annunzio, F.D. Victorelli, M.L. Frade, P.S. Ferreira, M. Chorilli, C.R. Fontana, Chitosan-based drug delivery systems for optimization of photodynamic therapy: a review, AAPS PharmSciTech 20 (2019) 253, https://doi.org/10.1208/s12249-019-1407-y.
[182] Z. Fan, C. Zhuang, S. Wang, Y. Zhang, Photodynamic and photothermal therapy of hepatocellular carcinoma, Front. Oncol. 11 (2021) 787780, https://doi.org/10.3389/fonc.2021.787780.
[183] A. Hak, M.S. Ali, S.A. Sankaranarayanan, V.R. Shinde, A.K. Rengan, Chlorin e6: a promising photosensitizer in photo-based cancer nanomedicine, ACS Appl. Bio Mater. 6 (2023) 349–364, https://doi.org/10.1021/acsabm.2c00891.
[184] J. Chen, W. Wu, F. Zhang, J. Zhang, H. Liu, J. Zheng, S. Guo, J. Zhang, Graphene quantum dots in photodynamic therapy, Nanoscale Adv. 2 (2020) 4961–4967, https://doi.org/10.1039/D0NA00631A.
[185] A. Zarepour, A. Khosravi, N. Yücel Ayten, P. Çakır Hatır, S. Iravani, A. Zarrabi, Innovative approaches for cancer treatment: graphene quantum dots for photodynamic and photothermal therapies, J. Mater. Chem. B 12 (2024) 4307–4334, https://doi.org/10.1039/D4TB00255E.
[186] T.K.W. Lee, X.Y. Guan, S. Ma, Cancer stem cells in hepatocellular carcinoma — from origin to clinical implications, Nat. Rev. Gastroenterol. Hepatol. 19 (2021) 26–44, https://doi.org/10.1038/s41575-021-00508-3.
[187] A. Barzegar Behrooz, A. Syahir, S. Ahmad, CD133: beyond a cancer stem cell biomarker, J. Drug Target. 27 (2019) 257–269, https://doi.org/10.1080/1061186X.2018.1479756.
[188] D.S. Mandlik, S.K. Mandlik, H.B. Choudhary, Immunotherapy for hepatocellular carcinoma: current status and future perspectives, World J. Gastroenterol. 29 (2023) 1054–1075, https://doi.org/10.3748/wjg.v29.I6.1054.
[189] S. Paul, M.F. Konig, D.M. Pardoll, C. Bettegowda, N. Papadopoulos, K.M. Wright, S.B. Gabelli, M. Ho, A. van Elsas, S. Zhou, Cancer therapy with antibodies, Nat. Rev. Cancer 24 (2024) 399–426, https://doi.org/10.1038/s41568-024-00690-x.
[190] V. Cesarini, S.L. Appleton, V. de Franciscis, D. Catalucci, The recent blooming of therapeutic aptamers, Mol. Aspect. Med. 102 (2025) 101350, https://doi.org/10.1016/j.mam.2025.101350.
[191] B.-H. Moon, Y. Kim, S.-Y. Kim, Twenty years of anti-vascular endothelial growth factor therapeutics in neovascular age-related macular degeneration treatment, Int. J. Mol. Sci. 24 (2023) 13004, https://doi.org/10.3390/ijms241613004.
[192] C.J. Danzig, A.M. Khanani, A. Loewenstein, C5 inhibitor avacincaptad pegol treatment for geographic atrophy: a comprehensive review, Immunotherapy 16 (2024) 779–790, https://doi.org/10.1080/1750743X.2024.2368342.
[193] S. Thongchot, K. Aksonnam, P. Thuwajit, P.-T. Yenchitsomanus, C. Thuwajit, Nucleolin-based targeting strategies in cancer treatment: focus on cancer immunotherapy (Review), Int. J. Mol. Med. 52 (2023) 81, https://doi.org/10.3892/ijmm.2023.5284.
[194] P.J. Bates, E.M. Reyes-Reyes, M.T. Malik, E.M. Murphy, M.G. O'Toole, J.O. Trent, G-quadruplex oligonucleotide AS1411 as a cancer-targeting agent: uses and mechanisms, Biochim. Biophys. Acta Gen. Subj. 1861 (2017) 1414–1428, https://doi.org/10.1016/j.bbagen.2016.12.015.
[195] J.E. Rosenberg, R.M. Bambury, E.M. Van Allen, H.A. Drabkin, P.N. Lara, A. L. Harzstark, N. Wagle, R.A. Figlin, G.W. Smith, L.A. Garraway, T. Choueiri, F. Erlandsson, D.A. Laber, A phase II trial of AS1411 (a novel nucleolin-targeted DNA aptamer) in metastatic renal cell carcinoma, Invest. N. Drugs 32 (2014) 178–187, https://doi.org/10.1007/s10637-013-0045-6.
[196] X. Tong, L. Ga, J. Ai, Y. Wang, Progress in cancer drug delivery based on AS1411 oriented nanomaterials, J. Nanobiotechnol. 20 (2022) 57, https://doi.org/10.1186/s12951-022-01240-z.
[197] F.A. Giordano, J.P. Layer, S. Leonardelli, L.L. Friker, R. Turiello, D. Corvino, T. Zeyen, C. Schaub, W. Müller, E. Sperk, L.C. Schmeel, K. Sahm, C. Oster, S. Kebir, P. Hambsch, T. Pietsch, S. Bisdas, M. Platten, M. Glas, C. Seidel, U. Herrlinger, M. Hölzel, L-RNA aptamer-based CXCL12 inhibition combined with radiotherapy in newly-diagnosed glioblastoma: dose escalation of the phase I/II

GLORIA trial, Nat. Commun. 15 (2024) 4210, https://doi.org/10.1038/s41467-024-48416-9.

[198] D. Eulberg, A. Frömming, K. Lapid, A. Mangasarian, A. Barak, The prospect of tumor microenvironment-modulating therapeutical strategies, Front. Oncol. 12 (2022) 1070243, https://doi.org/10.3389/fonc.2022.1070243.

[199] R. Didarian, H.K. Ozbek, V.C. Ozalp, O. Erel, N. Yildirim-Tirgil, Enhanced SELEX platforms for aptamer selection with improved characteristics: a review, Mol. Biotechnol. (2024), https://doi.org/10.1007/s12033-024-01256-w.